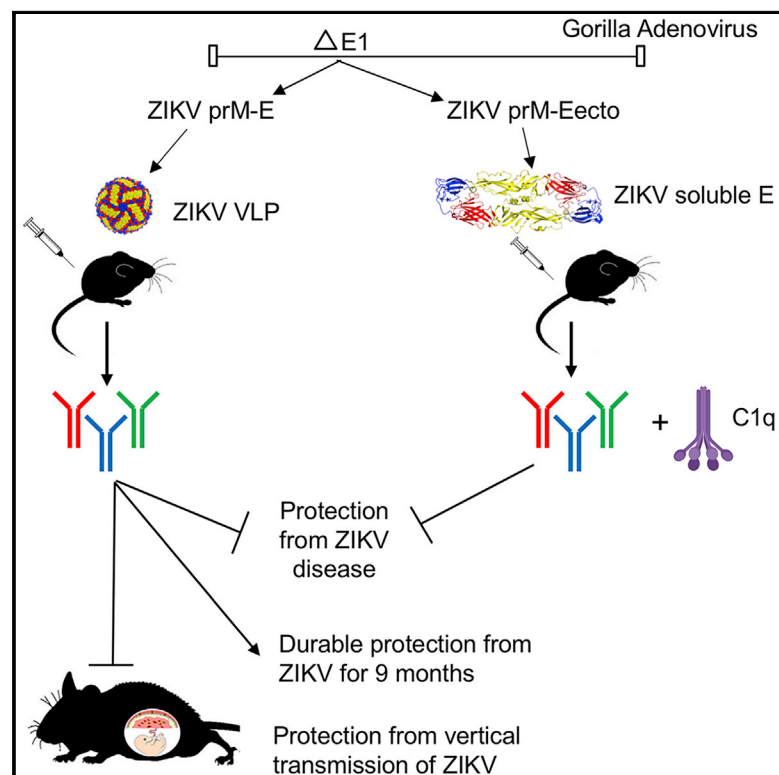Article

A Gorilla Adenovirus-Based Vaccine against Zika Virus Induces Durable Immunity and Confers Protection in Pregnancy

Graphical Abstract

Authors

Ahmed O. Hassan, Igor P. Dmitriev, Elena A. Kashentseva, ..., Daved H. Fremont, David T. Curiel, Michael S. Diamond

Correspondence

diamond@wusm.wustl.edu

In Brief

Hassan et al. generate gorilla adenovirus vector vaccines against ZIKV that induce durable neutralizing antibody responses and protect mice against lethal ZIKV challenge. One of the vaccines, which encodes for virus-like particles, protects against in utero transmission of ZIKV in immunocompromised and immunocompetent pregnancy models in mice.

Highlights

- ZIKV VLP and E protein vaccines are engineered using a gorilla adenovirus vector

- Both ZIKV vaccines protect mice against lethal ZIKV challenge

- ZIKV VLP vaccine induces durable protective immunity

- ZIKV VLP vaccine protects against congenital ZIKV infection in two pregnancy models

CellPress

A Gorilla Adenovirus-Based Vaccine against Zika Virus Induces Durable Immunity and Confers Protection in Pregnancy

Ahmed O. Hassan,[1] Igor P. Dmitriev,[2] Elena A. Kashentseva,[2] Haiyan Zhao,[3] Douglas E. Brough,[6] Daved H. Fremont,[3,4] David T. Curiel,[2] and Michael S. Diamond[1,3,4,5,7,*]

[1]Department of Medicine, Washington University School of Medicine, St. Louis, MO 63110, USA
[2]Department of Radiation Oncology, Washington University School of Medicine, St. Louis, MO 63110, USA
[3]Department of Pathology & Immunology, Washington University School of Medicine, St. Louis, MO 63110, USA
[4]Department of Molecular Microbiology, Washington University School of Medicine, St. Louis, MO 63110, USA
[5]The Andrew M. and Jane M. Bursky Center for Human Immunology and Immunotherapy Programs, Washington University School of Medicine, St. Louis, MO 63110, USA
[6]Precigen, 20358 Seneca Meadows Parkway, Germantown, MD 20876, USA
[7]Lead Contact
*Correspondence: diamond@wusm.wustl.edu
https://doi.org/10.1016/j.celrep.2019.08.005

SUMMARY

The teratogenic potential of Zika virus (ZIKV) has made the development of an effective vaccine a global health priority. Here, we generate two gorilla adenovirus-based ZIKV vaccines that encode for pre-membrane (prM) and envelope (E) proteins (GAd-Zvp) or prM and the ectodomain of E protein (GAd-Eecto). Both vaccines induce humoral and cell-mediated immune responses and prevent lethality after ZIKV challenge in mice. Protection is antibody dependent, CD8+ T cell independent, and for GAd-Eecto requires the complement component C1q. Immunization of GAd-Zvp induces antibodies against a key neutralizing epitope on domain III of E protein and confers durable protection as evidenced by memory B and long-lived plasma cell responses and challenge studies 9 months later. In two models of ZIKV infection during pregnancy, GAd-Zvp prevents maternal-to-fetal transmission. The gorilla adenovirus-based vaccine platform encoding full-length prM and E genes is a promising candidate for preventing congenital ZIKV syndrome and possibly infection by other flaviviruses.

INTRODUCTION

Zika virus (ZIKV) was isolated in Uganda in 1947 (Dick, 1952) and for decades remained restricted to African and Asian countries where sporadic human infections were reported (Jan et al., 1978; Olson et al., 1981). However, during the past decade, large-scale ZIKV epidemics have occurred in the Yap Islands, French Polynesia, and the Americas (Cao-Lormeau et al., 2014; Duffy et al., 2009; Roth et al., 2014). African and Asian lineages of ZIKV exist and comprise a single serotype (Dowd et al., 2016a). ZIKV isolates of the Asian lineage are responsible for recent epidemics in Oceania and the Americas (Berthet et al., 2014; Enfissi et al., 2016).

While infections historically cause a mild, self-limiting febrile illness accompanied by arthralgia, myalgia, rash, and headache (Zanluca et al., 2015), since its emergence in the Western hemisphere in 2015, ZIKV has become a global public health problem because infections during pregnancy caused microcephaly, developmental anomalies, or miscarriage of fetuses (van der Eijk et al., 2016; Mlakar et al., 2016; Pierson and Diamond, 2018). ZIKV infection in adults also is linked to the development of Guillain-Barré syndrome (GBS), a debilitating autoimmune disorder that affects peripheral nervous system function (Brasil et al., 2016; Cao-Lormeau et al., 2016; Oehler et al., 2014). Although ZIKV is spread principally by *Aedes aegypti* mosquitos (Boorman and Porterfield, 1956), other transmission routes have been described. Sexual transmission of ZIKV, with the ability to persist in vaginal secretions and semen for months, has been documented (Foy et al., 2011; Musso et al., 2015), and vertical transmission from infected mothers to fetuses causes congenital Zika syndrome (CZS) (Besnard et al., 2014; Mlakar et al., 2016).

ZIKV is an enveloped virus, with an 11-kilobase positive-sense RNA that is translated into a polyprotein composed of three structural (capsid [C], pre-membrane [prM], and envelope [E]) and seven non-structural (NS1, NS2A, NS2B, NS3, NS4A, 2K, NS4B, and NS5) proteins (Kuno and Chang, 2007). ZIKV virions form in the lumen of the endoplasmic reticulum as an immature virion composed of 60 prM-E heterotrimers (Prasad et al., 2017). The expression of prM is required for the biogenesis of ZIKV virions or virus-like particles (VLPs) (Roby et al., 2015); secreted VLPs are encoded by the full-length prM and E genes and can form during infection or when expressed in isolation (Allison et al., 1995). In the acidic environment of the Golgi network, a furin-mediated protease cleavage of prM occurs, and the pr peptide is released in the extracellular space, which results in the generation of a mature, infectious virion or VLP. The ectodomain of the ZIKV E protein is composed of three domains (DI, DII and DIII) and the target of most neutralizing antibodies and vaccines (Diamond et al., 2019; Richner and Diamond, 2018).
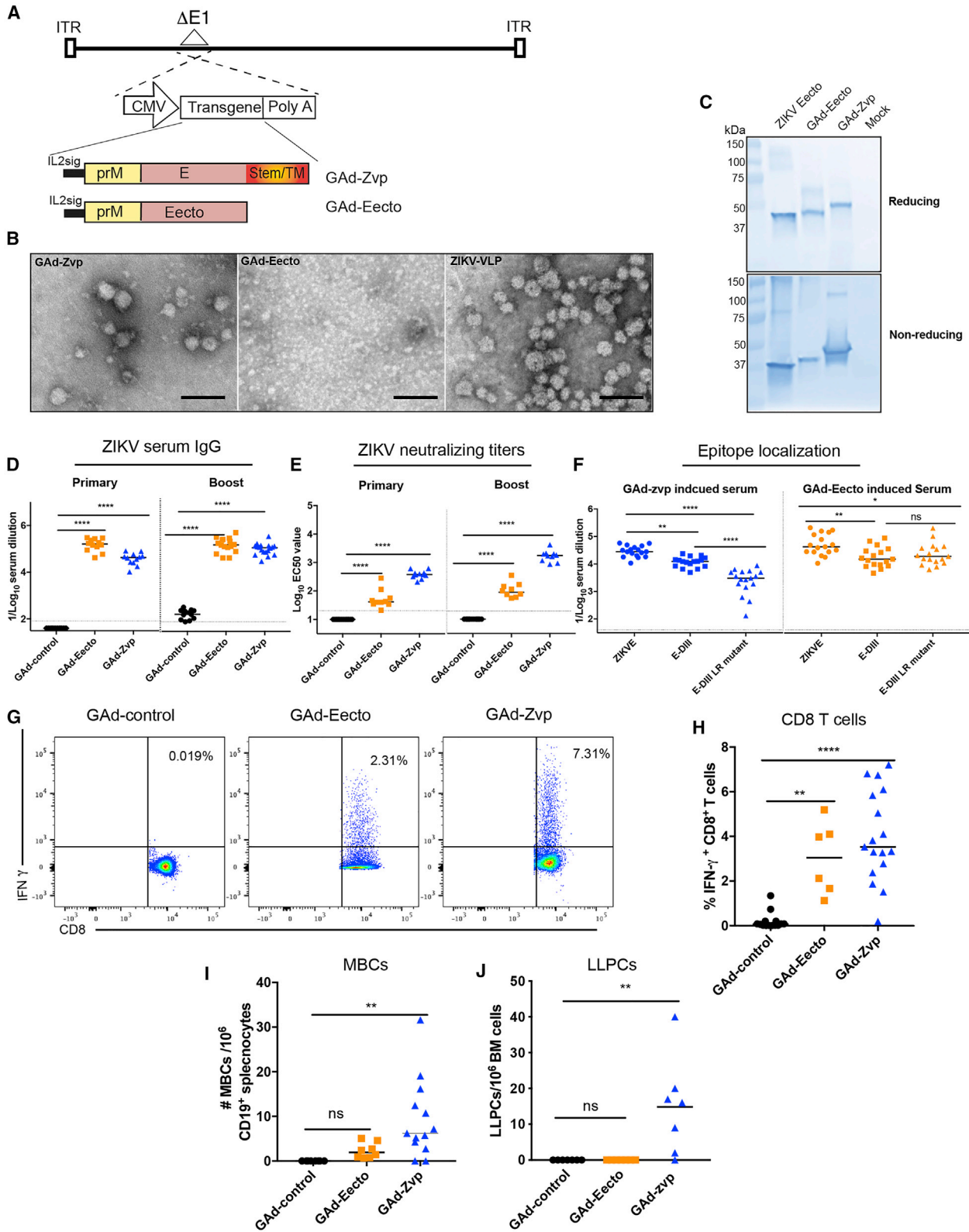
Because of its impact on global public health, substantial effort has been made toward developing vaccines against ZIKV, although none yet have been approved and only some have advanced to clinical testing in humans. Several vaccine platforms have been evaluated including DNA plasmids (Dowd et al., 2016b; Larocca et al., 2016), inactivated virions (Abbink et al., 2016; Larocca et al., 2016), modified mRNA (Pardi et al., 2017; Richner et al., 2017a), VLPs (Boigard et al., 2017), and viral vectors (Abbink et al., 2017; Emanuel et al., 2018; Nürnberger et al., 2019). Adenovirus-vectored vaccines, including human adenovirus (hAd5)-based vectors, represent a promising platform for multiple pathogens, as they offer excellent safety profiles and scalability for industrial production and induce robust and balanced immune responses (Wold and Toth, 2013). Nevertheless, two major limitations are associated with their use: (1) pre-existing immune responses to hAd5 can blunt immunity to the transgene, as hAd5 seroprevalence reaches to 35%–50% in human populations (Barouch et al., 2011; Nwanegbo et al., 2004; Xiang et al., 2006); and (2) while Ad5 and chimpanzee adenovirus type 3 (ChAd3) induce robust immune responses against encoded transgenes, other adenoviruses have been less immunogenic (Abbink et al., 2007; Colloca et al., 2012; Geisbert et al., 2011; Stanley et al., 2014).

Adenovirus-based vaccines against ZIKV have been evaluated. A rhesus monkey adenovirus (RhAd52) encoding for the M and E (but lacking the pr component) proteins induced protective immunity against ZIKV in mice and non-human primates (NHP) (Abbink et al., 2016; Larocca et al., 2016). A chimpanzee adenovirus (ChAd7) encoding for the M and E proteins protected mice against testicular damage (Xu et al., 2018), and a human adenovirus type 26 (Ad26) expressing ZIKV M and E proteins protected in mice and NHP (Cox et al., 2018). Incorporation of the full prM gene with E in human adenovirus type 2 (hAd2) backbone enhanced immunogenicity compared to hAd2 expressing only ZIKV E (Liu et al., 2018). Despite these promising results, none of the adenovirus-based vaccines against ZIKV have

been tested in animal models to prevent in utero transmission during pregnancy. However, passive protection was observed in challenged pups (at day 7 post-birth) of dams immunized with an hAd5 expressing ZIKV E fused to the T4 fibritin foldon trimerization domain (Kim et al., 2016).

Gorilla adenoviruses (GAd) have potential as a vectored vaccine platform (Johnson et al., 2014; Limbach et al., 2017) since less than 6% of US population shows seropositivity (Johnson et al., 2014). Indeed, a GAd-based vaccine against malaria was more effective than an Ad5-vectored vaccine (Limbach et al., 2017). Here, we describe the development of GAd that encode for the full-length prM and E proteins (GAd-Zvp) or prM and a truncated E protein (GAd-Eecto) of an Asian genotype ZIKV strain. Although both vaccines were immunogenic and conferred protection in a lethal challenge model of ZIKV infection, GAd-Zvp induced substantially higher levels of neutralizing antibodies. A single dose of GAd-Zvp induced durable B and T cell immunity and prevented maternal-to-fetal transmission of ZIKV in both immunocompromised and immunocompetent mice.

RESULTS

GAd-Eecto and GAd-Zvp Induce Anti-ZIKV Antibody Responses

We constructed three E1-deleted, replication defective GAds: GAd-control, GAd-Eecto, and GAd-Zvp containing no transgene, prM-E ectodomain of Asian strain H/PF/2013 (amino acids 123–696, sequence ID AHZ13508.1), and full-length prM-E (amino acids 123–794), respectively, with the target genes inserted under the transcriptional control of a cytomegalovirus (CMV) promoter in place of the deleted E1 gene (Figure 1A). The prM-E ectodomain construct results into a soluble form of E protein alone, whereas the prM-E full-length protein assembles into a VLP (Garg et al., 2017; Yang et al., 2017). The production of ZIKV VLPs in the supernatants of A549 cells infected with

Figure 1. Immunogenicity of GAd-ZIKV Vaccines in WT C57BL/6 Mice
(A) Schematic representation of the transgene cassettes. GAd-control has no transgene insert, whereas GAd-Eecto and GAd-Zvp contain ZIKV (strain H/PF/2013) a full prM-E cassette or prM-E ectodomain, respectively.
(B) A549 cells were infected with GAd-Eecto or GAd-Zvp followed by concentration of the supernatants by ultracentrifugation, negative staining, and transmission electron microscopy imaging to confirm the production of VLPs. High-power images are shown and compared to ZIKV VLP preparation generated by transfection of prM-E genes. Scale bar, 100 nm.
(C) ZIKV E protein expression in GAd-Eecto or GAd-Zvp. A549 cells were infected with GAd-Eecto, GAd-Zvp, or mock-infected, and supernatants were prepared and run on SDS-PAGE under reducing (upper blot) or non-reducing (lower blot) conditions along with recombinant ZIKV E ectodomain protein followed by detection using ZV-48. One representative blot from three experiments is shown.
(D–H) C57BL/6 mice were immunized with 10^9 viral particles of GAd-control, GAd-Eecto, or GAd-Zvp via intramuscular inoculation and boosted 3 weeks later.
(D and E) Humoral responses were evaluated in the sera of immunized mice at day 21 post-prime and day 21 post-boost. An ELISA measured ZIKV E-specific binding IgG (D), and a FRNT determined neutralization activity (EC_{50} values are shown) (E). Data for humoral responses are pooled from two experiments with n = 10–18 per group (ANOVA with a Dunnett's post-test comparing vaccine and control groups: ****p < 0.0001).
(F) Localization of GAd-Zvp and GAd-Eecto-induced polyclonal antibodies from sera. Binding to ZIKV Eecto, DIII, or DIII-LR mutant (A310E and T335K) was determined by ELISA from sera obtained post-boost at day 42 (n = 17 per group, ANOVA with a Tukey's post-test: ns, not significant; *p < 0.05; **p < 0.01; ****p < 0.0001).
(G–J) Cell-mediated immune responses were analyzed at 90–110 days post-initial immunization. Splenocytes were assayed for IFN-γ^+ ZIKV E-specific $CD8^+$ T cells using intracellular staining after peptide restimulation. Representative flow cytometry plots of four experiments are shown with percentages of IFN-γ^+ ZIKV-specific $CD8^+$ T cells (G). Summary of frequencies of IFN-γ^+ ZIKV-specific $CD8^+$ T cells are shown (H). ZIKV E-specific MBCs per million $CD19^+$ cells obtained from the spleen were determined by ELISA and Poisson distribution analysis (see STAR Methods) (I). An ELISPOT determined the number of ZIKV-specific IgG producing LLPCs per million bone marrow cells (J). Bars indicate median values per vaccine group. Data for cell mediated responses are pooled from four experiments with n = 6–17 animal per group (ANOVA with a Dunnett's post-test comparing vaccine and control groups: ns, not significant; **p < 0.01; ***p < 0.001). In this figure, dotted lines represent the limit of detection (LOD) of the assays.

GAd-Zvp but not GAd-Eecto was confirmed by electron microscopy (Figure 1B). Furthermore, E protein expression was confirmed in the supernatants of GAd-Zvp- or GAd-Eecto-infected A549 cells by western blotting with an anti-ZIKV E protein monoclonal antibody (mAb ZV-48; Zhao et al., 2016; Figure 1C). To evaluate the immunogenicity of GAd-Eecto and GAd-Zvp in immunocompetent mice, 8-week-old C57BL/6 mice were vaccinated by intramuscular inoculation with 10^9 virus particles of GAd-Eecto, GAd-Zvp, or GAd-control. Three weeks later, mice were boosted with a second dose of the same vaccine. Serum samples were collected at 3 weeks post-primary immunization and at 3 weeks post-booster immunization. An ELISA with ZIKV E protein was used to determine virus-specific immunoglobulin G (IgG) responses. Both GAd-Eecto and GAd-Zvp induced high levels of ZIKV E-specific IgG compared to the control vector (Figure 1D), with reciprocal mean endpoint titers of $171,732 \pm 87,886$ and $42,842 \pm 21,977$ after a single immunization, respectively. The ZIKV E-specific IgG titers were boosted slightly with the second dose of GAd-Eecto and GAd-Zvp (mean titers of $189,414 \pm 126,876$ and $118,826 \pm 73,022$, respectively). To assess the levels of neutralizing antibodies, focus-reduction neutralization tests (FRNT) were performed. Whereas a single dose of either vaccine induced neutralizing antibody against ZIKV (Figure 1E), the levels were higher for GAd-Zvp (mean effective half maximal inhibitory concentration [EC_{50}] of 396 ± 126) than GAd-Eecto (EC_{50} of 71 ± 78.5). Although a booster dose of GAd-Zvp augmented neutralization titers (EC_{50} of $1,796 \pm 919$), only a small increase was observed after the GAd-Eecto boost (EC_{50} of 113 ± 94).

Neutralizing antibodies isolated from ZIKV-infected individuals recognize epitopes on DI/II, DIII, E dimer epitopes, and quaternary epitopes formed by adjacent E proteins (Fernandez et al., 2017; Robbiani et al., 2017; Sapparapu et al., 2016; Stettler et al., 2016). DIII-specific mAbs have potently neutralizing activity against ZIKV (Robbiani et al., 2017; Sapparapu et al., 2016; Stettler et al., 2016; Wang et al., 2017), and those binding to the lateral ridge epitope (DIII-LR) efficiently protect mice against ZIKV challenge (Zhao et al., 2016). We evaluated whether the GAd-Eecto and GAd-Zvp vaccines differentially induced DIII-LR-specific antibodies by performing parallel binding assays with Eecto, DIII, or a DIII-LR mutant protein, the latter of which encodes for loss-of-binding substitutions (A310E and T335K) in the N-terminal region and BC loop of the epitope and abrogates binding of several neutralizing mAbs (Zhao et al., 2016). Three weeks after boosting (day 42), similar levels of polyclonal antibody against Eecto and DIII proteins were detected in sera from the two vaccines (Figure 1F). Remarkably, polyclonal antibodies from GAd-Zvp- but not GAd-Eecto-vaccinated mice exhibited diminished binding to the DIII-LR mutant compared to DIII protein. Thus, the antibody response of GAd-Zvp uniquely was skewed toward the neutralizing DIII-LR epitope.

Vaccine-Induced Memory B and T Cell Responses against ZIKV

To evaluate whether the GAd vaccines induced memory CD8+ T cell responses, mice were immunized and boosted as described above, and splenocytes were harvested on days 90–110 after initial immunization. Splenic CD8+ T cells were stained for intracellular expression of interferon (IFN)-γ after *ex vivo* restimulation with an H-2D^b-restricted immunodominant peptide (amino acids 294–302) in the ZIKV E protein (Elong Ngono et al., 2017). IFN-γ producing ZIKV E-specific CD8+ T cells were detected after immunization with GAd-Eecto ($3.0\% \pm 1.6$) or GAd-Zvp ($4.8\% \pm 2.3$) but not with the GAd control vector (Figures 1G and 1H).

We also assessed the ability of the GAd vaccines to induce ZIKV-specific memory responses in the B cell compartment. CD19+ memory B cells (MBCs) from GAd-vaccinated and boosted mice at days 90–110 after initial immunization were enriched from bulk splenocytes and then co-cultured for 6 days with NIH 3T3 feeder cells ectopically expressing CD40L, BAFF, and interleukin-21 (IL-21). Subsequently, supernatants from MBCs were harvested, the levels of ZIKV E-specific IgG were measured by ELISA, and the frequency of ZIKV E-specific MBCs was determined by Poisson distribution (Purtha et al., 2011). Both GAd-Zvp and GAd-Eecto induced ZIKV-specific MBCs, although only the levels induced by GAd-Zvp attained statistical significance compared to GAd-control vector (Figure 1I). Long-lived plasma cells (LLPCs), which principally reside in the bone marrow, constitutively secrete high levels of antibody and are the source of virus-specific IgG in circulation at times remote from infection or vaccination (Manz et al., 1997). To evaluate the LLPC response after vaccination, CD138+ bone marrow cells were harvested at days 90–110 and assayed for ZIKV E-specific IgG production by ELISPOT. ZIKV E-specific LLPCs were detected in the BM of GAd-Zvp-vaccinated mice but not in GAd-Eecto or GAd-control-vaccinated mice (Figure 1J).

GAd-Eecto and GAd-Zvp Protect Mice against ZIKV Lethal Challenge

C57BL/6 mice were immunized and boosted as described above with GAd-Eecto, GAd-Zvp, or GAd-control vaccines. At day 45 post-initial immunization (24 days after boosting), animals were challenged with 3×10^5 focus-forming units (FFUs) of a heterologous African strain of ZIKV strain (Dakar 41525) (Figure 2A), which is more pathogenic in mice than the H/PF/2013 ZIKV strain (Gorman et al., 2018; Lazear et al., 2016). One day prior to virus inoculation, mice were treated with a single 2 mg dose of anti-Ifnar1 blocking antibody (MAR1-5A3) (Sheehan et al., 2006) to facilitate a lethal ZIKV challenge model (Sapparapu et al., 2016). Mice vaccinated with GAd-Eecto or GAd-Zvp were fully protected against ZIKV-induced death, whereas those immunized with the control GAd vector had a 75% mortality rate (Figure 2B). At day 3 after ZIKV challenge, serum samples were analyzed for viremia. At this time point, there was no detectable viremia in any of the GAd-Zvp-vaccinated mice. In comparison, the majority (6 of 9) mice immunized with GAd-Eecto had measurable viremia (Figure 2C), although this was lower than in mice given the GAd-control vaccine. To assess whether GAd-Zvp induced sterilizing immunity, antibody responses against the non-structural protein NS1 were evaluated at day 9 after ZIKV challenge, as a measure of ZIKV replication post-challenge. Lower titers of anti-NS1 antibody titers were detected in GAd-Zvp mice compared to GAd-control or GAd-Eecto immunized mice (Figure 2D). Thus, while GAd-Zvp protected against ZIKV viremia and disease, it did not achieve sterilizing immunity.
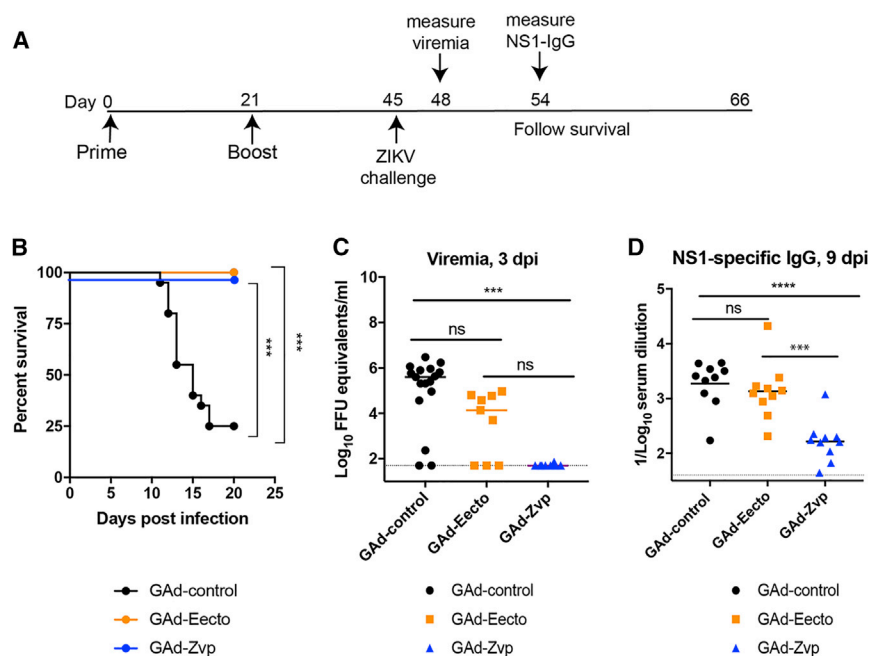
Figure 2. GAd-Eecto and GAd-Zvp Protect Mice against Lethal ZIKV Challenge

Eight-week-old C57BL/6 female mice were immunized with 10^9 viral particles of GAd-control (n = 20), GAd-Eecto (n = 10), or GAd-Zvp (n = 10) and boosted with a homologous dose 3 weeks later. On day 45 post-initial immunization, mice were challenged subcutaneously with 3×10^5 FFUs of ZIKV Dakar 41525 that was preceded by a single 2 mg anti-Ifnar1 mAb treatment 1 day prior to ZIKV infections.

(A) The experimental scheme of vaccination and challenge.

(B) Mice were monitored for mortality for 21 days following viral challenge (log-rank test with Bonferroni correction: ***p < 0.001).

(C) At day 3 after ZIKV challenge, serum was collected and assayed for viral RNA using RT-qPCR. The dotted line indicates the LOD of the assay. Data are pooled from two experiments with n = 9–20 mice per group (Kruskal-Wallis ANOVA with Dunn's post-test: ns, not significant; ***p < 0.001).

(D) An ELISA was used to measure serum anti-NS1 antibody responses obtained at day 9 after ZIKV challenge (n = 10 per group, ANOVA with a Tukey's post-test: ns, not significant; ***p < 0.001; ****p < 0.0001). In this figure, bars indicate median values and dotted lines represent the limit of detection (LOD) of the assays.

Mechanism of Vaccine Protection

To investigate the contribution of $CD8^+$ T cell responses to vaccine-mediated protection, cell depletion studies were performed. C57BL/6 mice were immunized with GAd-Eecto, GAd-Zvp, or GAd-control and boosted at day 21. At day 56 post-initial immunization, mice were challenged with 3×10^5 FFUs of ZIKV Dakar 41525 and monitored for survival. Mice were treated with 500 μg of depleting anti-CD8 or isotype control antibody on days −7, −3, +1, +5, and +12. One day prior to ZIKV challenge, mice also were inoculated with a single dose of 2 mg anti-Ifnar1 blocking antibody (MAR1-5A3). At day 7 post-infection, mice were bled and $CD8^+$ T cell depletion was confirmed in blood using flow cytometry (Figure 3A). Notably, both $CD8^+$ T cell-sufficient and depleted mice that were vaccinated with GAd-Eecto or GAd-Zvp survived lethal ZIKV challenge (Figure 3B), indicating a subordinate role for $CD8^+$ T cells in GAd vaccine-induced protective immunity. In comparison, in the GAd-control-vaccinated group, $CD8^+$ T cell-depleted mice (18 out of 19) fared slightly worse than $CD8^+$ T cell-sufficient mice (11 of 15) (Figure 3B), consistent with an established role of $CD8^+$ T cells in protection against primary ZIKV infection in mice (Elong Ngono et al., 2017; Huang et al., 2017; Winkler et al., 2017).

We performed passive transfer studies to define the contribution of antibody to vaccine-mediated protection. Sera (100 μL) from GAd-Eecto, GAd-Zvp, or GAd-control-vaccinated mice (obtained post-boost, at day 42) were transferred to naive C57BL/6 mice at day −1, concurrent with inoculation of a single dose of anti-Ifnar1 blocking antibody (MAR1-5A3). At day 0, mice were challenged with ZIKV Dakar 41525. Infected mice that received serum from GAd-Zvp- or GAd-Eecto-immunized

mice were completely protected against mortality (Figure 3C) with no weight loss observed (Figure 3D). In comparison, and as expected, mice receiving serum from GAd-control-treated mice succumbed to ZIKV infection with substantial weight loss and mortality. Thus, the humoral immune responses to GAd-Eecto and GAd-Zvp is sufficient to protect against lethal ZIKV challenge. Given the differences in neutralizing activity in serum from GAd-Eecto and GAd-Zvp mice (see Figure 1D), the equivalent levels of protection in the passive transfer experiments were unexpected. While this could reflect the relative dosing of sera tested, we hypothesized that the complement component C1q might augment the inhibitory activity of antibodies derived from GAd-Eecto immunization by reducing the stoichiometric threshold for neutralization (Mehlhop et al., 2009; Pierson et al., 2007). Indeed, in cell-culture experiments, addition of soluble, purified C1q enhanced the neutralizing activity of serum from GAd-Eecto immunized mice (Figure 3E). Based on these results, we repeated passive transfer experiments in $C1q^{-/-}$ mice. Whereas $C1q^{-/-}$ mice receiving serum from GAd-Zvp-immunized animals remained protected (Figure 3F), those given serum from GAd-Eecto- or GAd-control-immunized mice succumbed to ZIKV infection with a 100% mortality rate. Thus, antibodies present in GAd-Eecto immune sera required C1q and possibly other complement components for protection *in vivo*.

GAd-Zvp Induces Durable Protective Immunity

For GAd-Zvp, our best vaccine candidate, we assessed the durability and protective efficacy of humoral responses either after priming only at day 0 or a two-dose priming and boost (at day 21) regimen. FRNT assays were performed to evaluate
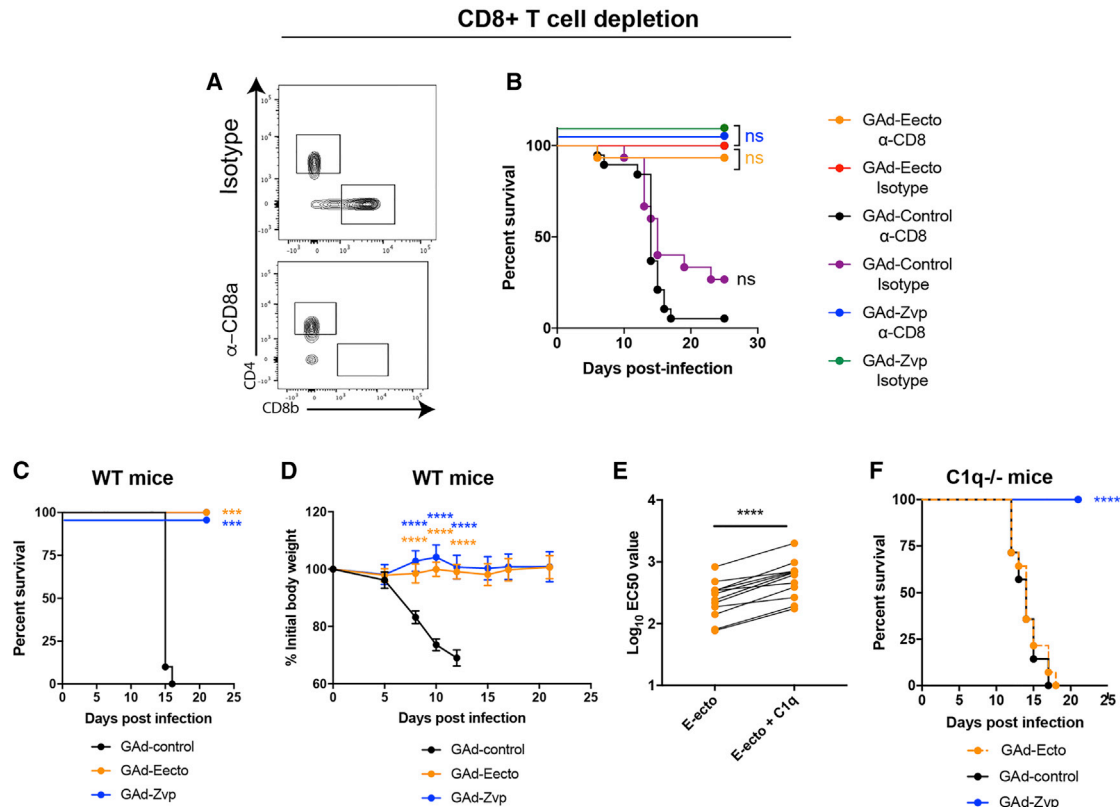
Figure 3. Mechanism of GAd-Eecto- and GAd-Zvp-Mediated Protection

(A and B) Effect of CD8$^+$ T cell depletion on protection mediated by GAd-Eecto or GAd-Zvp. Six-week-old C57BL/6 mice were immunized with 1 × 10^9 vp of GAd-Eecto (n = 30), GAd-Zvp (n = 20), or GAd-control (n = 35). Three weeks later, a homologous dose of each vaccine was administered to each group of mice. Mice were then treated with 500 μg of depleting anti-CD8 or isotype control antibody on days −7, −3, +1, +5, and +12. At day 0, mice were challenged subcutaneously with 3 × 10^5 FFUs of ZIKV Dakar 41525 that was preceded by a single 2 mg anti-Ifnar1 mAb treatment 1 day prior to infection. At day +7, mice were bled, and depletion of CD8$^+$ T cells was confirmed in PBMCs by flow cytometry (A). After ZIKV challenge, mice were monitored for mortality (B) (log-rank test with Bonferroni correction; CD8$^+$ T cell-depleted mice were compared to the isotype-control mAb-treated mice in the same vaccine group: ns, not significant). Data are pooled from two experiments (n = 20–35 animals per vaccine group).

(C, D, and F) Serum samples collected at day 45 from mice that received two doses of GAd-control, GAd-Eecto, or GAd-Zvp were passively transferred to 10- to 12-week-old wild-type mice (n = 10 per group) or congenic $C1q^{-/-}$ (n = 9–17 animals per group) mice 1 day prior to challenge with 3 × 10^5 FFUs of ZIKV Dakar 41525 following anti-Ifnar1 mAb treatment. Wild-type mice were followed for mortality (C) and weight change (D), while $C1q^{-/-}$ mice were only followed for mortality (F). Data are pooled from three experiments (survival analysis: log-rank test with Bonferroni correction: ***p < 0.001; ****p < 0.0001; weight change analysis: two-way ANOVA with a Sidak's post-test to compare vaccine groups relative to control group: ****p < 0.0001).

(E) Serum samples collected at day 45 from mice that received two doses of GAd-Eecto were evaluated by FRNT with or without addition of exogenous complement protein C1q. EC$_{50}$ values are shown and were analyzed for differences using a paired t test (****p < 0.0001).

ZIKV neutralizing antibody titers, and ELISA was conducted to assess ZIKV E-specific binding antibody titers. ZIKV neutralizing antibody titers induced by GAd-Zvp single immunization were elevated at 10 weeks post-immunization (EC$_{50}$ of 1,206 ± 865), peaked at 18 weeks post-immunization (EC$_{50}$ of 2,168 ± 1378), and then waned slightly at 38 weeks post-immunization (Figure 4A). A similar trend was observed with ZIKV E-specific IgG (Figure 4B), with reciprocal mean endpoint titers of 167,523 ± 110,941, 108,783 ± 50,306, and 52,923 ± 51,398 at 10, 18, and 38 weeks after a single immunization, respectively. In comparison, two immunizations induced higher levels of neutralizing antibodies at 10 weeks post-initial immunization (EC$_{50}$ of 3,029 ± 1,604) that declined at 18 (EC$_{50}$ of 2,200 ± 1,757) and 38 weeks (EC$_{50}$ of 402 ± 237) post-initial immunization (Figure 4C). ZIKV E-specific

IgG, however, remained more stable after two immunizations (Figure 4D), with mean titers of 110,582 ± 55,508, 148,188 ± 60,419, and 106,644 ± 39,268 at 10, 18, and 38 weeks post-initial immunization, respectively.

To assess the durability of protective efficacy of GAd-Zvp, mice were immunized with the same regimens described above and then challenged with a lethal dose of ZIKV Dakar 41525 at 10, 18, or 38 weeks post-initial immunization. One day prior to ZIKV infection, mice were treated with a single dose of anti-Ifnar1 mAb. All mice that received one or two immunizations of GAd-Zvp exhibited no weight loss and survived lethal ZIKV challenge at 10, 18, and 38 weeks, whereas most of the GAd-control-vaccinated mice succumbed to ZIKV infection with significant weight loss observed (Figures 4E–4P).
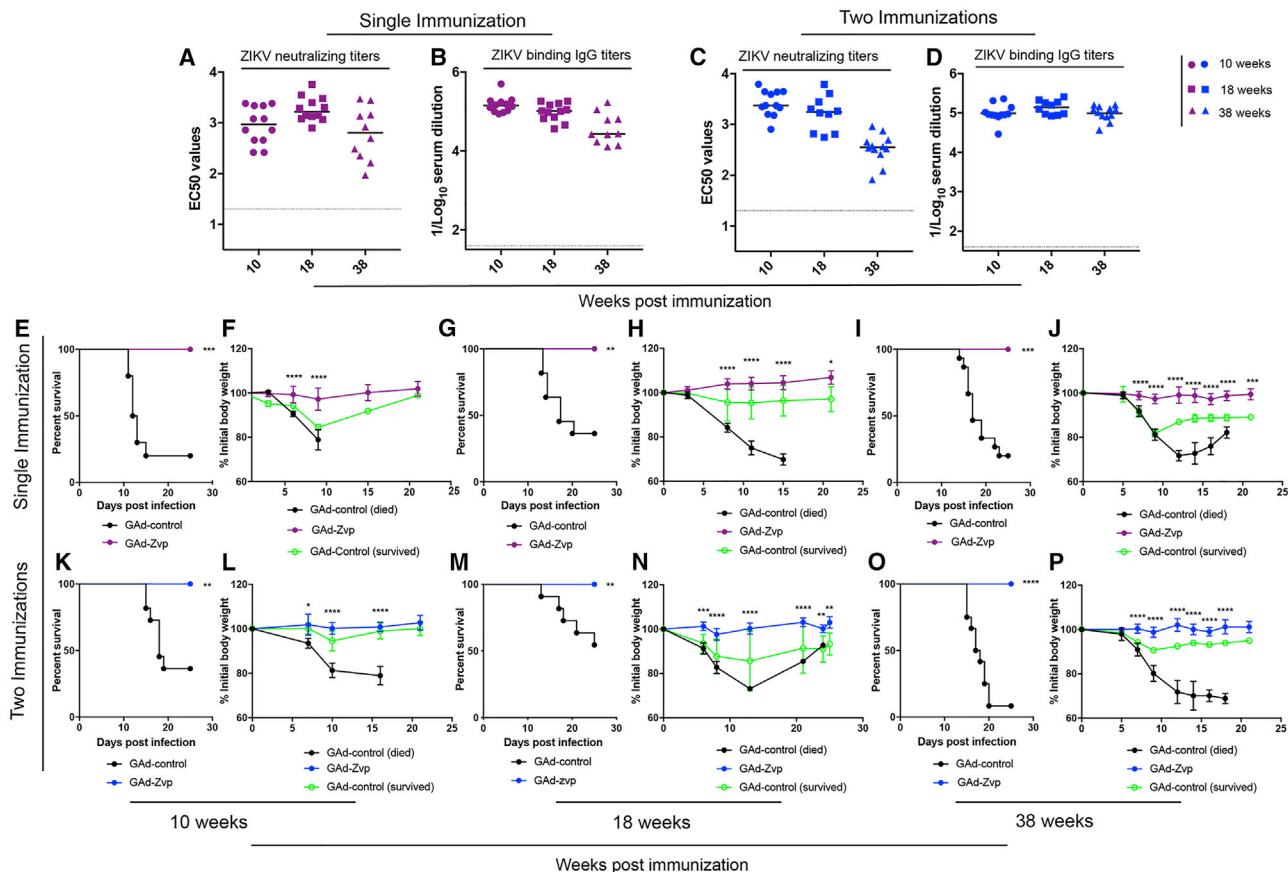
Figure 4. GAd-Zvp Induces Durable Protective Immunity

C57BL/6 mice received one or two doses of GAd-Zvp or GAd-control.

(A–D) Humoral immune responses were evaluated in the sera of immunized mice at 10, 18, and 38 weeks post-initial immunization. An ELISA measured ZIKV E-specific binding IgG (B and D), and a FRNT determined neutralization activity (EC$_{50}$ values are shown; A and C). Humoral responses data are pooled from two experiments with n = 6–12 per group.

(E–P) Mice that were immunized with one or two doses of GAd-Zvp or GAd-control were challenged with 3 × 10^5 FFUs of ZIKV Dakar 41525 following anti-Ifnar1 mAb treatment at 10, 18, and 38 weeks post-initial immunization (n = 10–12 mice per group) (survival analysis: log-rank test followed by Bonferroni correction: **p < 0.01; ***p < 0.001; ****p < 0.0001; weight change analysis: two-way ANOVA with Sidak's post-test correction: *p < 0.05; **p < 0.01; ***p < 0.001; ****p < 0.0001). Dotted lines represent the LOD of the assays, and bars indicate the median values.

GAd-Zvp Protects Pregnant Mice and Their Fetuses against ZIKV Infection

As ZIKV causes congenital anomalies in fetuses from mothers infected during pregnancy, a key property of a ZIKV vaccine will be its ability to protect against vertical transmission. We used both immunocompromised and immunocompetent mouse models of ZIKV challenge to assess the efficacy of GAd-Zvp during pregnancy (Figure 5A). In the immunocompromised mouse model, 4-week-old C57BL/6 female mice were immunized with either GAd-Zvp or GAd-control vaccines by intramuscular inoculation. A homologous booster vaccine dose was administered 21 days later. At day 49 (4 weeks post-boost), immunized females were mated with males and monitored for vaginal plugs. At embryo day 5 (E5), pregnant females were administered a single 2 mg dose of anti-Ifnar1, to facilitate virus dissemination to the placenta (Richner et al., 2017b). At E6, the pregnant females were challenged with 3 × 10^5 FFUs of ZIKV Dakar 41525. Mice were euthanized at E13, and maternal and fetal organs were har-

vested for viral burden analysis. In maternal, placental, and fetal tissues from the majority of GAd-Zvp immunized dams, there was little or no detectable viral RNA (Figures 5B–5E). However, one GAd-Zvp-vaccinated dam showed breakthrough, with ZIKV RNA present in the placenta and fetal heads, although the levels were substantially reduced (20,800- and 12,800-fold in the placenta and fetal head, respectively) compared to GAd-control-treated dams.

For the immunocompetent challenge model during pregnancy, hSTAT2-KI C57BL/6 mice were used (Gorman et al., 2018); in this transgenic mouse, human *STAT2* replaces mouse *Stat2*, which allows ZIKV to overcome a species restriction barrier and evade IFN signaling cascades in infected cells (Grant et al., 2016). Four-week-old hSTAT2-KI females were immunized and boosted with GAd-Zvp or GAd-control vaccines by intramuscular inoculation according to the described scheme (Figure 5A). Twelve-week-old hSTAT2-KI females were mated with hSTAT2-KI males and monitored for vaginal plugs. At E6
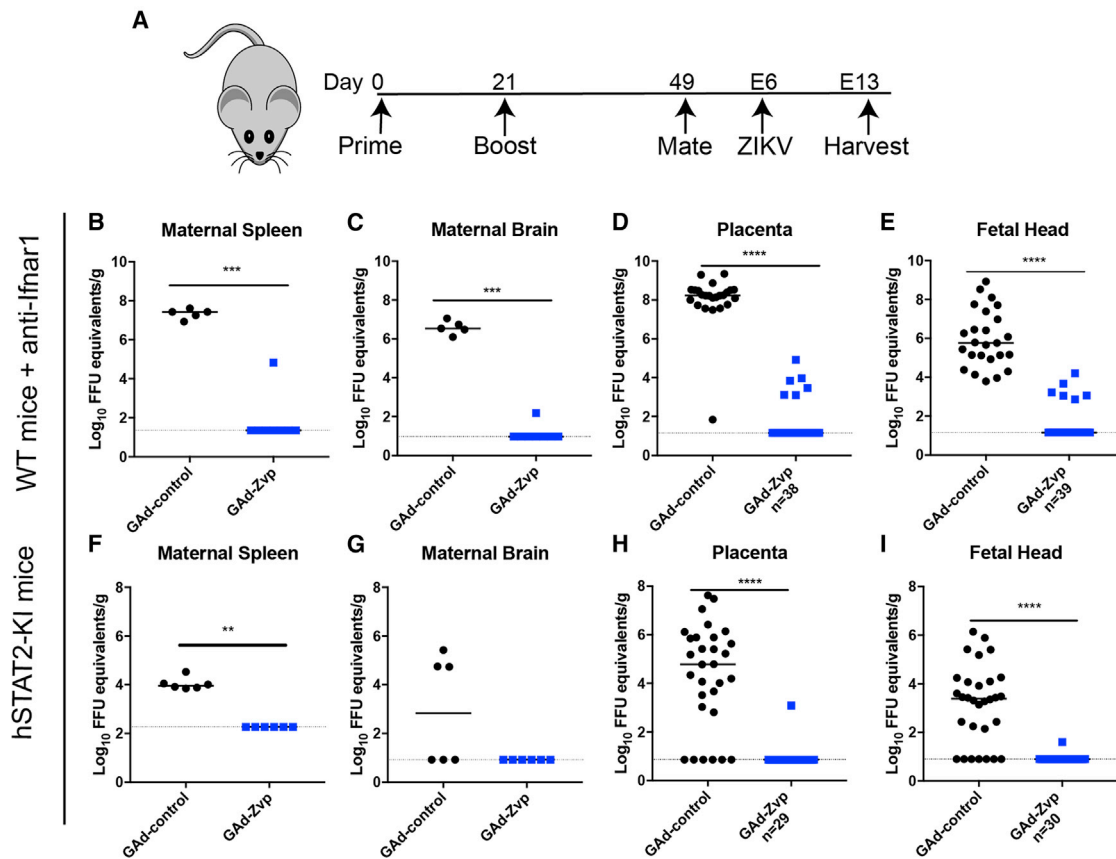
Figure 5. GAd-Zvp Protects Pregnant Mice and Their Fetuses against ZIKV Infection

(A) Representation of the immunization and infection scheme.

(B–E) Immunized 12- to 13-week-old wild-type C57BL/6 female mice were mated with wild-type C57BL/6 males. At E5, pregnant mice were given a single 2 mg dose of anti-Ifnar1 mAb. At E6, pregnant mice were inoculated with 3×10^5 FFUs of ZIKV Dakar 41525 by a subcutaneous route. At day E13, mice were euthanized and maternal spleen (B), maternal brain (C), placenta (D), and fetal heads (E) were harvested and assayed for ZIKV RNA levels.

(F–I) Immunized 11- to 12-week-old hSTAT2-KI C57BL/6 female mice were challenged with 3×10^5 FFUs of ZIKV Dakar 41525 by a subcutaneous route. Mice were euthanized at day E13 and maternal spleen (F), maternal brain (G), placenta (H), and fetal heads (I) were harvested and assayed for ZIKV RNA levels. Dotted lines indicate the LOD of the assays, and bars represent median values. Data are from at least three experiments, with the following number of pregnant mice analyzed: wild-type + anti-Ifnar1 mAb treatment; GAd-control, n = 5; GAd-Zvp, n = 8; hSTAT2-KI mice; n = 6 for GAd-control or GAd-Zvp. The numbers of placenta and fetal heads analyzed are indicated in the figure. Statistical significance was determined by a Mann-Whitney test: **p < 0.01; ***p < 0.001; ****p < 0.0001.

(approximately 5 weeks post-boosting), pregnant hSTAT2-KI females were challenged with 3×10^5 FFUs of ZIKV Dakar 41525. At E13, mice were euthanized, and maternal and fetal organs were harvested. With the exception of a breakthrough in one placenta and its associated fetus, the remainder of placental and fetal tissues from GAd-Zvp immunized dams were negative for viral RNA (Figures 5F–5I). In comparison, those vaccinated with GAd-control vaccine showed significant levels of infection in both fetal tissues.

DISCUSSION

The development of a ZIKV vaccine remains an urgent global public health need due to its deleterious effects on unborn fetuses of infected mothers. In the few years since the epidemic emerged, several vaccine candidates have been developed using multiple platforms including mRNA, inactivated virion, live-attenuated or chimeric virus, purified E protein, VLPs, and viral vectors-based ZIKV vaccines (Abbink et al., 2016; 2017; Cox et al. 2018; Dowd et al., 2016b; Emanuel et al., 2018; Kim et al., 2016; Li et al., 2018; Muthumani et al., 2016; Nürnberger et al., 2019; Pardi et al., 2017; Richner et al., 2017a, 2017b, Shan et al., 2017a, 2017b; Xu et al., 2018). Three DNA vaccines encoding ZIKV prM and E and one inactivated virus vaccine have completed evaluation in phase I trials in humans (Gaudinski et al., 2018; Modjarrad et al., 2018; Tebas et al., 2017). Although many of these vaccines have shown efficacy in pre-clinical challenge models, fewer studies have been performed in the context of vertical transmission, and none have used an immunocompetent mouse model with robust replication after peripheral inoculation (Gorman et al., 2018).

A GAd that was recently isolated has been developed as a vaccine vector for pathogens to overcome the pre-existing Ad5 immunity in humans (Brough, 2015; Duncan et al., 2013;

Johnson et al., 2014). We utilized this vector to develop vaccines expressing a soluble form of ZIKV E protein (GAd-Ecto) or the full-length prM-E proteins (GAd-Zvp), which assemble into VLPs (Garg et al., 2017; Yang et al., 2017). Both of our vaccine candidates induced neutralizing antibodies, although the titers achieved with GAd-Eecto were substantially less than GAd-Zvp. Epitope localization analysis revealed that GAd-Zvp preferentially induced antibodies that bound a key neutralizing epitope on the LR of DIII of E protein (Nybakken et al., 2005; Oliphant et al., 2005; Robbiani et al., 2017; Wang et al., 2017; Zhao et al., 2016), whereas GAd-Eecto did not. The basis for this difference in immunogenicity remains uncertain but could reflect the display of antigens on the multivalent VLP generated by expression of prM-E compared to the soluble E protein. Notwithstanding this idea, a measles-based ZIKV vaccine expressing soluble E protein appeared to generate high levels of neutralizing antibodies, although no comparisons with prM-E were attempted in that study (Nürnberger et al., 2019). One question that remains is whether neutralizing antibody responses to GAd-Zvp in humans would similarly target the DIII-LR epitope since for some flaviviruses (e.g., West Nile virus [WNV] and Dengue virus [DENV]) this epitope is more immunodominant in mice than in humans (Beltramello et al., 2010; Oliphant et al., 2007). Although epitope-based analysis of human antibody responses to the GAd-Zvp ultimately will be required to address this question, several highly protective human DIII-LR antibodies have been isolated against natural ZIKV infection (Robbiani et al., 2017; Sapparapu et al., 2016; Wang et al., 2017, 2016). These results suggest that humans can make protective DIII-LR-specific antibodies in response to ZIKV structural protein antigens. Despite the differences in humoral response, both GAd-Eecto and GAd-Zvp vaccines protected against lethal ZIKV challenge in mice. A single GAd-Zvp immunization resulted in durable protection in mice even nine months later, with only a slight decline in neutralizing antibody titers. Finally, GAd-Zvp demonstrated marked protection against maternal-to-fetal transmission of ZIKV in two different mouse models, with the vast majority of fetuses showing no evidence of infection.

Several human and nonhuman adenovirus-based ZIKV vaccines have been evaluated. A single dose of RhAd52 expressing ZIKV M-E induced durable neutralizing immunity that conferred protection against challenge 1 year post-vaccination in rhesus monkeys. Moreover, passive transfer of purified IgG from rhesus monkeys at 1 year post-vaccination to mice resulted in protection against ZIKV challenge (Abbink et al., 2017). Similarly, Ad26 expressing the same ZIKV M-E transgene induced humoral and cellular immune responses and protected mice and NHPs against viremia upon ZIKV challenge (Cox et al., 2018). A hAd5 vaccine candidate expressing codon-optimized ZIKV M-E in which the transmembrane domain was replaced by a T4 fibritin foldon trimerization domain induced neutralizing antibodies in mice (Kim et al., 2016). This vaccine also protected pups of immunized dams that were infected with ZIKV at day 7 post-birth. A chimpanzee adenovirus (ChAd7) expressing ZIKV M and E proteins elicited neutralizing antibodies, T cell responses, and conferred protection against lethal virus challenge (Xu et al., 2018). A direct comparison of many of the published ZIKV vaccination platforms including their dosing, neutralizing activity, and

protection conferred in mice is summarized (Table S1). While the majority of studies with these vectored and other subunit, inactivated, or live-attenuated vaccine platforms evaluated serum antibody titers after immunization, none interrogated long-term MBC responses. Moreover, only a few other ZIKV vaccines have established protection against congenital transmission during pregnancy (Nürnberger et al., 2019; Richner et al., 2017b; Shan et al., 2017b).

The GAd-Zvp vaccine effectively minimized vertical transmission during pregnancy in the immunocompromised challenge model. There was little, if any detectable viral RNA in the placental and fetal tissues with the exception of breakthrough in one of the dams, and, even then, the levels of infection were much lower than in GAd-control-treated dams. Similar levels of GAd-Zvp-mediated protection were seen in the immunized immunocompetent hSTAT2-KI mice. The clinical significance of the low levels of viral RNA in the placenta and fetus that occurred in the context of vaccine breakthrough remains unknown. Moreover, these events occurred in the setting of detectable neutralizing antibody, as seen previously with modified mRNA or live-attenuated ZIKV vaccines (Richner et al., 2017b; Shan et al., 2017b). The mechanistic basis for this breakthrough in the setting of neutralizing antibody warrants further studies but could reflect virus that is transmitted by cells in blood rather than in plasma (Michlmayr et al., 2017).

Many animal experiments have established that vaccine-induced or passively transferred neutralizing antibodies represent a correlate of protection against flavivirus infection (Belmusto-Worn et al., 2005; Ben-Nathan et al., 2003; Diamond et al., 2003; Engle and Diamond, 2003; Heinz et al., 2007; Mason et al., 1973; Swanstrom et al., 2016). Indeed, several studies with ZIKV vaccines have suggested that neutralizing antibodies are a likely correlate of protection (Abbink et al., 2016; Dowd et al., 2016b; Larocca et al., 2016; Richner et al., 2017a; Sapparapu et al., 2016). Passive transfer of serum from GAd-Eecto and GAd-Zvp immunized mice was sufficient to confer protection against lethal ZIKV challenge in mice. However, when passive transfer experiments were repeated in $C1q^{-/-}$ mice, serum from GAd-Zvp- but not GAd-Eecto-immunized mice conferred protection. This finding suggests that the protection provided by the GAd-Ecto-induced antibodies, which are less neutralizing, is complement dependent and is consistent with the concept that C1q binding to the Fc region of antibody reduces the stoichiometric threshold of neutralization and improves antibody protection against flaviviruses (Mehlhop et al., 2009). The lower neutralizing antibody response observed with GAd-Eecto may be due to the different presentation of E protein epitopes. Whereas GAd-Zvp, which encodes for full-length prM and E, produces VLPs, GAd-Eecto produces a soluble form of E protein. VLPs are multivalent, repetitive antigen structures that morphologically resemble infectious virions but lack viral RNA and capsid (Allison et al., 1995; Rodríguez-Limas et al., 2013). The more potent antibody responses associated with particulate VLPs also could be explained by (1) the ability of particles of this size to traffic to lymph nodes, bind to follicular dendritic cells, and induce primary antibody responses (Reddy et al., 2006); (2) efficient binding of VLPs to IgM and complement with subsequent presentation of VLPs antigens to B cells in the lymph nodes (Link et al., 2012); and (3) VLPs induce potent T helper responses as a

result of efficient uptake and processing by antigen-presenting cells (Bachmann and Jennings, 2010). Although antigen-specific CD8^{+} T cell responses also were generated upon immunization and have been shown protective during primary ZIKV infection (Elong Ngono et al., 2017; Huang et al., 2017; Winkler et al., 2017), depletion studies suggest they had a subordinate role in GAd vaccine-mediated immunity.

A single dose of GAd-Zvp induced a durable immune response that protected mice against lethal ZIKV challenge 9 months later. The durable IgG response likely is produced by LLPCs, which reside in the bone marrow and continuously secrete antibodies into circulation independently of antigen exposure (Amanna and Slifka, 2010). Although GAd-Zvp induced a robust LLPC response, GAd-Eecto did not appear to. This could be attributed to the nature of the antigen produced in each vaccine. The repetitive arrangement of envelope proteins on the surface of VLPs produced by GAd-Zvp likely facilitates enhanced recognition by B cells (Metz and Pijlman, 2016) and transmission of a potent activation signal (Jegerlehner et al., 2002) that could influence differentiation of LLPCs.

In summary, we have shown that immunization with GAd-Zvp resulted in robust and durable neutralizing antibody responses as well as cellular immune responses including antigen-specific CD8^{+} T cells, MBCs, and LLPCs. A single immunization of GAd-Zvp was sufficient to confer durable protection against lethal ZIKV challenge and two doses conferred protection against vertical transmission of ZIKV in pregnant mice in two different models. Given the safety profiles of recombinant adenovirus vectors established in hundreds of clinical trials, the scalable manufacturing of millions of doses using approved cell lines, the low seroprevalence of GAd that overcomes pre-existing hAd5 immunity, and finally the efficacy of preclinical evaluation shown in this study, GAd-Zvp is a promising vaccine candidate that warrants further evaluation.

STAR★METHODS

Detailed methods are provided in the online version of this paper and include the following:

- KEY RESOURCES TABLE
- LEAD CONTACT AND MATERIALS AVAILABILITY
- EXPERIMENTAL MODEL AND SUBJECT DETAILS
  - Viruses and cells
  - Mouse experiments
- METHOD DETAILS
  - Construction and generation of GAd vectors
  - Negative staining and transmission electron microscopy
  - ELISA
  - Neutralization assay
  - MBC limiting dilution assay
  - ELISPOT assay
  - Measurement of viral burden
  - Intracellular Cytokine Staining
  - CD8^{+} T cell depletion
- QUANTIFICATION AND STATISTICAL ANALYSIS
- DATA AND CODE AVAILABILITY

REFERENCES

Abbink, P., Lemckert, A.A.C., Ewald, B.A., Lynch, D.M., Denholtz, M., Smits, S., Holterman, L., Damen, I., Vogels, R., Thorner, A.R., et al. (2007). Comparative seroprevalence and immunogenicity of six rare serotype recombinant adenovirus vaccine vectors from subgroups B and D. J. Virol. 81, 4654–4663.

Abbink, P., Larocca, R.A., De La Barrera, R.A., Bricault, C.A., Moseley, E.T., Boyd, M., Kirilova, M., Li, Z., Nganga, D., Nanayakkara, O., et al. (2016). Protective efficacy of multiple vaccine platforms against Zika virus challenge in rhesus monkeys. Science 353, 1129–1132.

Abbink, P., Larocca, R.A., Visitsunthorn, K., Boyd, M., Barrera, La, R.A.D., Gromowski, G.D., Kirilova, M., Peterson, R., Li, Z., Nanayakkara, O., et al. (2017). Durability and correlates of vaccine protection against Zika virus in rhesus monkeys. Sci. Transl. Med. 9, eaao4163.

Allison, S.L., Stadler, K., Mandl, C.W., Kunz, C., and Heinz, F.X. (1995). Synthesis and secretion of recombinant tick-borne encephalitis virus protein E in soluble and particulate form. J. Virol. 69, 5816–5820.

Amanna, I.J., and Slifka, M.K. (2006). Quantitation of rare memory B cell populations by two independent and complementary approaches. J. Immunol. Methods 317, 175–185.

Amanna, I.J., and Slifka, M.K. (2010). Mechanisms that determine plasma cell lifespan and the duration of humoral immunity. Immunol. Rev. 236, 125–138.

Bachmann, M.F., and Jennings, G.T. (2010). Vaccine delivery: a matter of size, geometry, kinetics and molecular patterns. Nat. Publ. Gr. 10, 787–796.

Baronti, C., Piorkowski, G., Charrel, R.N., Boubis, L., Leparc-Goffart, I., and de Lamballerie, X. (2014). Complete coding sequence of Zika Virus from a French Polynesia outbreak in 2013. Genome Announc. 2, e00500-14. https://doi.org/10.1128/genomeA.00500-14.

Barouch, D.H., Kik, S.V., Weverling, G.J., Dilan, R., King, S.L., Maxfield, L.F., Clark, S., Ng'ang'a, D., Brandariz, K.L., Abbink, P., et al. (2011). International seroepidemiology of adenovirus serotypes 5, 26, 35, and 48 in pediatric and adult populations. Vaccine 29, 5203–5209.

Belmusto-Worn, V.E., Sanchez, J.L., McCarthy, K., Nichols, R., Bautista, C.T., Magill, A.J., Pastor-Cauna, G., Echevarria, C., Laguna-Torres, V.A., Samame, B.K., et al. (2005). Randomized, double-blind, phase III, pivotal field trial of the

comparative immunogenicity, safety, and tolerability of two yellow fever 17D vaccines (Arilvax and YF-VAX) in healthy infants and children in Peru. Am. J. Trop. Med. Hyg. 72, 189–197.

Beltramello, M., Williams, K.L., Simmons, C.P., Macagno, A., Simonelli, L., Quyen, N.T.H., Sukupolvi-Petty, S., Navarro-Sanchez, E., Young, P.R., de Silva, A.M., et al. (2010). The human immune response to Dengue virus is dominated by highly cross-reactive antibodies endowed with neutralizing and enhancing activity. Cell Host Microbe 8, 271–283.

Ben-Nathan, D., Lustig, S., Tam, G., Robinzon, S., Segal, S., and Rager-Zisman, B. (2003). Prophylactic and therapeutic efficacy of human intravenous immunoglobulin in treating West Nile virus infection in mice. J. Infect. Dis. 188, 5–12.

Berthet, N., Nakouné, E., Kamgang, B., Selekon, B., Descorps-Declère, S., Gessain, A., Manuguerra, J.C., and Kazanji, M. (2014). Molecular characterization of three Zika flaviviruses obtained from sylvatic mosquitoes in the Central African Republic. Vector Borne Zoonotic Dis. 14, 862–865.

Besnard, M., Lastere, S., Teissier, A., Cao-Lormeau, V., and Musso, D. (2014). Evidence of perinatal transmission of Zika virus, French Polynesia, December 2013 and February 2014. Euro Surveill. 19, 20751.

Boigard, H., Alimova, A., Martin, G.R., Katz, A., Gottlieb, P., and Galarza, J.M. (2017). Zika virus-like particle (VLP) based vaccine. PLoS Negl. Trop. Dis. 11, e0005608.

Boorman, J.P., and Porterfield, J.S. (1956). A simple technique for infection of mosquitoes with viruses; transmission of Zika virus. Trans. R. Soc. Trop. Med. Hyg. 50, 238–242.

Botto, M., Dell'Agnola, C., Bygrave, A.E., Thompson, E.M., Cook, H.T., Petry, F., Loos, M., Pandolfi, P.P., and Walport, M.J. (1998). Homozygous C1q deficiency causes glomerulonephritis associated with multiple apoptotic bodies. Nat. Genet. 19, 56–59.

Brasil, P., Sequeira, P.C., Freitas, A.D., Zogbi, H.E., Calvet, G.A., de Souza, R.V., Siqueira, A.M., de Mendonca, M.C.L., Nogueira, R.M.R., de Filippis, A.M.B., and Solomon, T. (2016). Guillain-Barré syndrome associated with Zika virus infection. Lancet 387, 1482.

Brough, D.E. (2015). Gorilla Adenovirus Vectors for Molecular Therapeutics and Vaccines. Mol. Ther. 23, S23.

Cao-Lormeau, V.M., Roche, C., Teissier, A., Robin, E., Berry, A.L., Mallet, H.P., Sall, A.A., and Musso, D. (2014). Zika virus, French polynesia, South pacific, 2013. Emerg. Infect. Dis. 20, 1085–1086.

Cao-Lormeau, V.M., Blake, A., Mons, S., Lastère, S., Roche, C., Vanhomwegen, J., Dub, T., Baudouin, L., Teissier, A., Larre, P., et al. (2016). Guillain-Barré Syndrome outbreak associated with Zika virus infection in French Polynesia: a case-control study. Lancet 387, 1531–1539.

Colloca, S., Barnes, E., Folgori, A., Ammendola, V., Capone, S., Cirillo, A., Siani, L., Naddeo, M., Grazioli, F., Esposito, M.L., et al. (2012). Vaccine vectors derived from a large collection of simian adenoviruses induce potent cellular immunity across multiple species. Sci. Transl. Med. 4, 115ra2.

Cox, F., Van Der Fits, L., Abbink, P., Larocca, R.A., Van Huizen, E., Saeland, E., Verhagen, J., Peterson, R., Tolboom, J., Kaufmann, B., et al. (2018). Adenoviral vector type 26 encoding Zika virus (ZIKV) M-Env antigen induces humoral and cellular immune responses and protects mice and nonhuman primates against ZIKV challenge. PLoS One 13, e0202820.

Diamond, M.S., Shrestha, B., Marri, A., Mahan, D., and Engle, M. (2003). B cells and antibody play critical roles in the immediate defense of disseminated infection by West Nile encephalitis virus. J. Virol. 77, 2578–2586.

Diamond, M.S., Ledgerwood, J.E., and Pierson, T.C. (2019). Zika Virus Vaccine Development: Progress in the Face of New Challenges. Annu. Rev. Med. 70, 121–135.

Dick, G.W. (1952). Zika virus. II. Pathogenicity and physical properties. Trans. R. Soc. Trop. Med. Hyg. 46, 521–534.

Dowd, K.A., DeMaso, C.R., Pelc, R.S., Speer, S.D., Smith, A.R.Y., Goo, L., Platt, D.J., Mascola, J.R., Graham, B.S., Mulligan, M.J., et al. (2016a). Broadly Neutralizing Activity of Zika Virus-Immune Sera Identifies a Single Viral Serotype. Cell Rep. 16, 1485–1491.

Dowd, K.A., Ko, S.Y., Morabito, K.M., Yang, E.S., Pelc, R.S., DeMaso, C.R., Castilho, L.R., Abbink, P., Boyd, M., Nityanandam, R., et al. (2016b). Rapid development of a DNA vaccine for Zika virus. Science 354, 237–240.

Duffy, M.R., Chen, T.H., Hancock, W.T., Powers, A.M., Kool, J.L., Lanciotti, R.S., Pretrick, M., Marfel, M., Holzbauer, S., Dubray, C., et al. (2009). Zika virus outbreak on Yap Island, Federated States of Micronesia. N. Engl. J. Med. 360, 2536–2543.

Duncan, M., Cranfield, M.R., Torano, H., Kuete, H.M., Lee, G.P., Glenn, A., Bruder, J.T., Rangel, D., Brough, D.E., and Gall, J.G. (2013). Adenoviruses isolated from wild gorillas are closely related to human species C viruses. Virology 444, 119–123.

Elong Ngono, A., Vizcarra, E.A., Tang, W.W., Sheets, N., Joo, Y., Kim, K., Gorman, M.J., Diamond, M.S., and Shresta, S. (2017). Mapping and Role of the CD8+ T Cell Response During Primary Zika Virus Infection in Mice. Cell Host Microbe 21, 35–46.

Emanuel, J., Callison, J., Dowd, K.A., Pierson, T.C., Feldmann, H., and Marzi, A. (2018). A VSV-based Zika virus vaccine protects mice from lethal challenge. Sci. Rep. 8, 11043.

Enfissi, A., Codrington, J., Roosblad, J., Kazanji, M., and Rousset, D. (2016). Zika virus genome from the Americas. Lancet 387, 227–228.

Engle, M.J., and Diamond, M.S. (2003). Antibody prophylaxis and therapy against West Nile virus infection in wild-type and immunodeficient mice. J. Virol. 77, 12941–12949.

Fernandez, E., Dejnirattisai, W., Cao, B., Scheaffer, S.M., Supasa, P., Wongwiwat, W., Esakky, P., Drury, A., Mongkolsapaya, J., Moley, K.H., et al. (2017). Human antibodies to the dengue virus E-dimer epitope have therapeutic activity against Zika virus infection. Nat. Immunol. 18, 1261–1269.

Foy, B.D., Kobylinski, K.C., Chilson Foy, J.L., Blitvich, B.J., Travassos da Rosa, A., Haddow, A.D., Lanciotti, R.S., and Tesh, R.B. (2011). Probable non-vector-borne transmission of Zika virus, Colorado, USA. Emerg. Infect. Dis. 17, 880–882.

Gall, J.G.D., Lizonova, A., EttyReddy, D., McVey, D., Zuber, M., Kovesdi, I., Aughtman, B., King, C.R., and Brough, D.E. (2007). Rescue and production of vaccine and therapeutic adenovirus vectors expressing inhibitory transgenes. Mol. Biotechnol. 35, 263–273.

Garg, H., Sedano, M., Plata, G., Punke, E.B., and Joshi, A. (2017). Development of Virus-Like-Particle Vaccine and Reporter Assay for Zika Virus. J. Virol. 91, e00834-17.

Gaudinski, M.R., Houser, K.V., Morabito, K.M., Hu, Z., Yamshchikov, G., Rothwell, R.S., Berkowitz, N., Mendoza, F., Saunders, J.G., Novik, L., et al.; VRC 319; VRC 320 study teams (2018). Safety, tolerability, and immunogenicity of two Zika virus DNA vaccine candidates in healthy adults: randomised, open-label, phase 1 clinical trials. Lancet 391, 552–562.

Geisbert, T.W., Bailey, M., Hensley, L., Asiedu, C., Geisbert, J., Stanley, D., Honko, A., Johnson, J., Mulangu, S., Pau, M.G., et al. (2011). Recombinant adenovirus serotype 26 (Ad26) and Ad35 vaccine vectors bypass immunity to Ad5 and protect nonhuman primates against ebolavirus challenge. J. Virol. 85, 4222–4233.

Gorman, M.J., Caine, E.A., Zaitsev, K., Begley, M.C., Weger-Lucarelli, J., Uccellini, M.B., Tripathi, S., Morrison, J., Yount, B.L., Dinnon, K.H., 3rd., et al. (2018). An Immunocompetent Mouse Model of Zika Virus Infection. Cell Host Microbe 23, 672–685.

Grant, A., Ponia, S.S., Tripathi, S., Balasubramaniam, V., Miorin, L., Sourisseau, M., Schwarz, M.C., Sánchez-Seco, M.P., Evans, M.J., Best, S.M., and García-Sastre, A. (2016). Zika Virus Targets Human STAT2 to Inhibit Type I Interferon Signaling. Cell Host Microbe 19, 882–890.

Heinz, F.X., Holzmann, H., Essl, A., and Kundi, M. (2007). Field effectiveness of vaccination against tick-borne encephalitis. Vaccine 25, 7559–7567.

Huang, H., Li, S., Zhang, Y., Han, X., Jia, B., Liu, H., Liu, D., Tan, S., Wang, Q., Bi, Y., et al. (2017). CD8+ T Cell Immune Response in Immunocompetent Mice during Zika Virus Infection. J. Virol. 91, 91.

Jan, C., Languillat, G., Renaudet, J., and Robin, Y. (1978). Bull. Soc. Pathol. Exot. 71, 140–146.

Jegerlehner, A., Storni, T., Lipowsky, G., Schmid, M., Pumpens, P., and Bachmann, M.F. (2002). Regulation of IgG antibody responses by epitope density and CD21-mediated costimulation. Eur. J. Immunol. 32, 3305–3314.

Johnson, T.R., Rangel, D., Graham, B.S., Brough, D.E., and Gall, J.G. (2014). Genetic vaccine for respiratory syncytial virus provides protection without disease potentiation. Mol. Ther. 22, 196–205.

Kim, E., Erdos, G., Huang, S., Kenniston, T., Falo, L.D., Jr., and Gambotto, A. (2016). Preventative Vaccines for Zika Virus Outbreak: Preliminary Evaluation. EBioMedicine 13, 315–320.

Kuno, G., and Chang, G.J.J. (2007). Full-length sequencing and genomic characterization of Bagaza, Kedougou, and Zika viruses. Arch. Virol. 152, 687–696.

Larocca, R.A., Abbink, P., Peron, J.P.S., Zanotto, P.M., Iampietro, M.J., Badamchi-Zadeh, A., Boyd, M., Ng'ang'a, D., Kirilova, M., Nityanandam, R., et al. (2016). Vaccine protection against Zika virus from Brazil. Nature 536, 474–478.

Lazear, H.M., Govero, J., Smith, A.M., Platt, D.J., Fernandez, E., Miner, J.J., and Diamond, M.S. (2016). A Mouse Model of Zika Virus Pathogenesis. Cell Host Microbe 19, 720–730.

Li, X.F., Dong, H.L., Wang, H.J., Huang, X.Y., Qiu, Y.F., Ji, X., Ye, Q., Li, C., Liu, Y., Deng, Y.Q., et al. (2018). Development of a chimeric Zika vaccine using a licensed live-attenuated flavivirus vaccine as backbone. Nat. Commun. 9, 673.

Limbach, K., Stefaniak, M., Chen, P., Patterson, N.B., Liao, G., Weng, S., Krepkiy, S., Ekberg, G., Torano, H., Ettyreddy, D., et al. (2017). New gorilla adenovirus vaccine vectors induce potent immune responses and protection in a mouse malaria model. Malar. J. 16, 263.

Link, A., Zabel, F., Schnetzler, Y., Titz, A., Brombacher, F., and Bachmann, M.F. (2012). Innate immunity mediates follicular transport of particulate but not soluble protein antigen. J. Immunol. 188, 3724–3733.

Liu, X., Qu, L., Ye, X., Yi, C., Zheng, X., Hao, M., Su, W., Yao, Z., Chen, P., Zhang, S., et al. (2018). Incorporation of NS1 and prM/M are important to confer effective protection of adenovirus-vectored Zika virus vaccine carrying E protein. NPJ Vaccines 3, 29.

Manz, R.A., Thiel, A., and Radbruch, A. (1997). Lifetime of plasma cells in the bone marrow. Nature 388, 133–134.

Mason, R.A., Tauraso, N.M., Spertzel, R.O., and Ginn, R.K. (1973). Yellow fever vaccine: direct challenge of monkeys given graded doses of 17D vaccine. Appl. Microbiol. 25, 539–544.

Mehlhop, E., Nelson, S., Jost, C.A., Gorlatov, S., Johnson, S., Fremont, D.H., Diamond, M.S., and Pierson, T.C. (2009). Complement protein C1q reduces the stoichiometric threshold for antibody-mediated neutralization of West Nile virus. Cell Host Microbe 6, 381–391.

Metz, S.W., and Pijlman, G.P. (2016). Production of Chikungunya Virus-Like Particles and Subunit Vaccines in Insect Cells. Methods Mol. Biol. 1426, 297–309.

Michlmayr, D., Andrade, P., Gonzalez, K., Balmaseda, A., and Harris, E. (2017). CD14+CD16+ monocytes are the main target of Zika virus infection in peripheral blood mononuclear cells in a paediatric study in Nicaragua. Nat. Microbiol. 2, 1462–1470.

Mittereder, N., March, K.L., and Trapnell, B.C. (1996). Evaluation of the concentration and bioactivity of adenovirus vectors for gene therapy. J. Virol. 70, 7498–7509.

Mlakar, J., Korva, M., Tul, N., Popović, M., Poljšak-Prijatelj, M., Mraz, J., Kolenc, M., Resman Rus, K., Vesnaver Vipotnik, T., Fabjan Vodušek, V., et al. (2016). Zika Virus Associated with Microcephaly. N. Engl. J. Med. 374, 951–958.

Modjarrad, K., Lin, L., George, S.L., Stephenson, K.E., Eckels, K.H., De La Barrera, R.A., Jarman, R.G., Sondergaard, E., Tennant, J., Ansel, J.L., et al. (2018). Preliminary aggregate safety and immunogenicity results from three trials of a purified inactivated Zika virus vaccine candidate: phase 1, randomised, double-blind, placebo-controlled clinical trials. Lancet 391, 563–571.

Musso, D., Roche, C., Robin, E., Nhan, T., Teissier, A., and Cao-Lormeau, V.M. (2015). Potential sexual transmission of Zika virus. Emerg. Infect. Dis. 21, 359–361.

Muthumani, K., Griffin, B.D., Agarwal, S., Kudchodkar, S.B., Reuschel, E.L., Choi, H., Kraynyak, K.A., Duperret, E.K., Keaton, A.A., Chung, C., et al. (2016). In vivo protection against ZIKV infection and pathogenesis through passive antibody transfer and active immunisation with a prMEnv DNA vaccine. NPJ Vaccines 1, 16021.

Nürnberger, C., Bodmer, B.S., Fiedler, A.H., Gabriel, G., and Mühlebach, M.D. (2019). A Measles Virus-Based Vaccine Candidate Mediates Protection against Zika Virus in an Allogeneic Mouse Pregnancy Model. J. Virol. 93, 93.

Nwanegbo, E., Vardas, E., Gao, W., Whittle, H., Sun, H., Rowe, D., Robbins, P.D., and Gambotto, A. (2004). Prevalence of neutralizing antibodies to adenoviral serotypes 5 and 35 in the adult populations of The Gambia, South Africa, and the United States. Clin. Diagn. Lab. Immunol. 11, 351–357.

Nybakken, G.E., Oliphant, T., Johnson, S., Burke, S., Diamond, M.S., and Fremont, D.H. (2005). Structural basis of West Nile virus neutralization by a therapeutic antibody. Nature 437, 764–769.

Oehler, E., Watrin, L., Larre, P., Leparc-Goffart, I., Lastere, S., Valour, F., Baudouin, L., Mallet, H., Musso, D., and Ghawche, F. (2014). Zika virus infection complicated by Guillain-Barre syndrome–case report, French Polynesia, December 2013. Euro Surveill. 19, 19.

Oliphant, T., Engle, M., Nybakken, G.E., Doane, C., Johnson, S., Huang, L., Gorlatov, S., Mehlhop, E., Marri, A., Chung, K.M., et al. (2005). Development of a humanized monoclonal antibody with therapeutic potential against West Nile virus. Nat. Med. 11, 522–530.

Oliphant, T., Nybakken, G.E., Engle, M., Xu, Q., Nelson, C.A., Sukupolvi-Petty, S., Marri, A., Lachmi, B.E., Olshevsky, U., Fremont, D.H., et al. (2006). Antibody recognition and neutralization determinants on domains I and II of West Nile Virus envelope protein. J. Virol. 80, 12149–12159.

Oliphant, T., Nybakken, G.E., Austin, S.K., Xu, Q., Bramson, J., Loeb, M., Throsby, M., Fremont, D.H., Pierson, T.C., and Diamond, M.S. (2007). Induction of epitope-specific neutralizing antibodies against West Nile virus. J. Virol. 81, 11828–11839.

Olson, J.G., Ksiazek, T.G., Suhandiman, and Triwibowo. (1981). Zika virus, a cause of fever in Central Java, Indonesia. Trans. R. Soc. Trop. Med. Hyg. 75, 389–393.

Pardi, N., Hogan, M.J., Pelc, R.S., Muramatsu, H., Andersen, H., DeMaso, C.R., Dowd, K.A., Sutherland, L.L., Scearce, R.M., Parks, R., et al. (2017). Zika virus protection by a single low-dose nucleoside-modified mRNA vaccination. Nature 543, 248–251.

Pierson, T.C., and Diamond, M.S. (2018). The emergence of Zika virus and its new clinical syndromes. Nature 560, 573–581.

Pierson, T.C., Xu, Q., Nelson, S., Oliphant, T., Nybakken, G.E., Fremont, D.H., and Diamond, M.S. (2007). The stoichiometry of antibody-mediated neutralization and enhancement of West Nile virus infection. Cell Host Microbe 1, 135–145.

Prasad, V.M., Miller, A.S., Klose, T., Sirohi, D., Buda, G., Jiang, W., Kuhn, R.J., and Rossmann, M.G. (2017). Structure of the immature Zika virus at 9 Å resolution. Nat. Struct. Mol. Biol. 24, 184–186.

Purtha, W.E., Tedder, T.F., Johnson, S., Bhattacharya, D., and Diamond, M.S. (2011). Memory B cells, but not long-lived plasma cells, possess antigen specificities for viral escape mutants. J. Exp. Med. 208, 2599–2606.

Reddy, S.T., Rehor, A., Schmoekel, H.G., Hubbell, J.A., and Swartz, M.A. (2006). In vivo targeting of dendritic cells in lymph nodes with poly(propylene sulfide) nanoparticles. J. Control. Release 112, 26–34.

Richner, J.M., and Diamond, M.S. (2018). Zika virus vaccines: immune response, current status, and future challenges. Curr. Opin. Immunol. 53, 130–136.

Richner, J.M., Himansu, S., Dowd, K.A., Butler, S.L., Salazar, V., Fox, J.M., Julander, J.G., Tang, W.W., Shresta, S., Pierson, T.C., et al. (2017a). Modified mRNA Vaccines Protect against Zika Virus Infection. Cell 169, 176.

Richner, J.M., Jagger, B.W., Shan, C., Fontes, C.R., Dowd, K.A., Cao, B., Himansu, S., Caine, E.A., Nunes, B.T.D., Medeiros, D.B.A., et al. (2017b). Vaccine Mediated Protection Against Zika Virus-Induced Congenital Disease. Cell 170, 273–283.

Robbiani, D.F., Bozzacco, L., Keeffe, J.R., Khouri, R., Olsen, P.C., Gazumyan, A., Schaefer-Babajew, D., Avila-Rios, S., Nogueira, L., Patel, R., et al. (2017). Recurrent Potent Human Neutralizing Antibodies to Zika Virus in Brazil and Mexico. Cell *169*, 597–609.e11.

Roby, J.A., Setoh, Y.X., Hall, R.A., and Khromykh, A.A. (2015). Post-translational regulation and modifications of flavivirus structural proteins. J. Gen. Virol. *96*, 1551–1569.

Rodríguez-Limas, W.A., Sekar, K., and Tyo, K.E. (2013). Virus-like particles: the future of microbial factories and cell-free systems as platforms for vaccine development. Curr. Opin. Biotechnol. *24*, 1089–1093.

Roth, A., Mercier, A., Lepers, C., Hoy, D., Duituturaga, S., Benyon, E., Guillaumot, L., and Souares, Y. (2014). Concurrent outbreaks of dengue, chikungunya and Zika virus infections - an unprecedented epidemic wave of mosquito-borne viruses in the Pacific 2012-2014. Euro Surveill. *19*, 19.

Sapparapu, G., Fernandez, E., Kose, N., Bin Cao, B., Fox, J.M., Bombardi, R.G., Zhao, H., Nelson, C.A., Bryan, A.L., Barnes, T., et al. (2016). Neutralizing human antibodies prevent Zika virus replication and fetal disease in mice. Nature *540*, 443–447.

Shan, C., Muruato, A.E., Nunes, B.T.D., Luo, H., Xie, X., Medeiros, D.B.A., Wakamiya, M., Tesh, R.B., Barrett, A.D., Wang, T., et al. (2017a). A live-attenuated Zika virus vaccine candidate induces sterilizing immunity in mouse models. Nat. Med. *23*, 763–767.

Shan, C., Muruato, A.E., Jagger, B.W., Richner, J., Nunes, B.T.D., Medeiros, D.B.A., Xie, X., Nunes, J.G.C., Morabito, K.M., Kong, W.P., et al. (2017b). A single-dose live-attenuated vaccine prevents Zika virus pregnancy transmission and testis damage. Nat. Commun. *8*, 676.

Sheehan, K.C.F., Lai, K.S., Dunn, G.P., Bruce, A.T., Diamond, M.S., Heutel, J.D., Dungo-Arthur, C., Carrero, J.A., White, J.M., Hertzog, P.J., and Schreiber, R.D. (2006). Blocking monoclonal antibodies specific for mouse IFN-α/β receptor subunit 1 (IFNAR-1) from mice immunized by in vivo hydrodynamic transfection. J. Interferon Cytokine Res. *26*, 804–819.

Stanley, D.A., Honko, A.N., Asiedu, C., Trefry, J.C., Lau-Kilby, A.W., Johnson, J.C., Hensley, L., Ammendola, V., Abbate, A., Grazioli, F., et al. (2014). Chimpanzee adenovirus vaccine generates acute and durable protective immunity against ebolavirus challenge. Nat. Med. *20*, 1126–1129.

Stettler, K., Beltramello, M., Espinosa, D.A., Graham, V., Cassotta, A., Bianchi, S., Vanzetta, F., Minola, A., Jaconi, S., Mele, F., et al. (2016). Specificity, cross-reactivity, and function of antibodies elicited by Zika virus infection. Science *353*, 823–826.

Swanstrom, J.A., Plante, J.A., Plante, K.S., Young, E.F., McGowan, E., Gallichotte, E.N., Widman, D.G., Heise, M.T., de Silva, A.M., and Baric, R.S. (2016). Dengue Virus Envelope Dimer Epitope Monoclonal Antibodies Isolated from Dengue Patients Are Protective against Zika Virus. MBio *7*, e01123–e16.

Tebas, P., Roberts, C.C., Muthumani, K., Reuschel, E.L., Kudchodkar, S.B., Zaidi, F.I., White, S., Khan, A.S., Racine, T., Choi, H., et al. (2017). Safety and Immunogenicity of an Anti–Zika Virus DNA Vaccine — Preliminary Report. N. Engl. J. Med. Published online October 4, 2017. https://doi.org/10.1056/NEJMoa1708120.

van der Eijk, A.A., van Genderen, P.J., Verdijk, R.M., Reusken, C.B., Mögling, R., van Kampen, J.J.A., Widagdo, W., Aron, G.I., GeurtsvanKessel, C.H., Pas, S.D., et al. (2016). Miscarriage Associated with Zika Virus Infection. N. Engl. J. Med. *375*, 1002–1004.

Wang, Q., Yang, H., Liu, X., Dai, L., Ma, T., Qi, J., Wong, G., Peng, R., Liu, S., Li, J., et al. (2016). Molecular determinants of human neutralizing antibodies isolated from a patient infected with Zika virus. Sci. Transl. Med. *8*, 369ra179.

Wang, J., Bardelli, M., Espinosa, D.A., Pedotti, M., Ng, T.S., Bianchi, S., Simonelli, L., Lim, E.X.Y., Foglierini, M., Zatta, F., et al. (2017). A Human Bi-specific Antibody against Zika Virus with High Therapeutic Potential. Cell *171*, 229–241.

Winkler, C.W., Myers, L.M., Woods, T.A., Messer, R.J., Carmody, A.B., McNally, K.L., Scott, D.P., Hasenkrug, K.J., Best, S.M., and Peterson, K.E. (2017). Adaptive Immune Responses to Zika Virus Are Important for Controlling Virus Infection and Preventing Infection in Brain and Testes. J. Immunol. *198*, 3526–3535.

Wold, W.S.M., and Toth, K. (2013). Adenovirus vectors for gene therapy, vaccination and cancer gene therapy. Curr. Gene Ther. *13*, 421–433.

Xiang, Z., Li, Y., Cun, A., Yang, W., Ellenberg, S., Switzer, W.M., Kalish, M.L., and Ertl, H.C.J. (2006). Chimpanzee adenovirus antibodies in humans, sub-Saharan Africa. Emerg. Infect. Dis. *12*, 1596–1599.

Xu, K., Song, Y., Dai, L., Zhang, Y., Lu, X., Xie, Y., Zhang, H., Cheng, T., Wang, Q., Huang, Q., et al. (2018). Recombinant Chimpanzee Adenovirus Vaccine AdC7-M/E Protects against Zika Virus Infection and Testis Damage. Jvi.Asm.Org 1. J. Virol. *92*, 1722–1739.

Yang, M., Lai, H., Sun, H., and Chen, Q. (2017). Virus-like particles that display Zika virus envelope protein domain III induce potent neutralizing immune responses in mice. Sci. Rep. *7*, 7679.

Zanluca, C., Melo, V.C., Mosimann, A.L.P., Santos, G.I., Santos, C.N., and Luz, K. (2015). First report of autochthonous transmission of Zika virus in Brazil. Mem. Inst. Oswaldo Cruz *110*, 569–572.

Zhao, H., Fernandez, E., Dowd, K.A., Speer, S.D., Platt, D.J., Gorman, M.J., Govero, J., Nelson, C.A., Pierson, T.C., Diamond, M.S., and Fremont, D.H. (2016). Structural Basis of Zika Virus-Specific Antibody Protection. Cell *166*, 1016–1027.

STAR★METHODS

KEY RESOURCES TABLE

REAGENT or RESOURCE	SOURCE	IDENTIFIER
Antibodies		
ZV-48	Diamond laboratory	Zhao et al., 2016
MAR1-5A3 (anti-IFNAR1)	Leinco	Cat # I-401
WNV E60 (anti-E, fusion loop specific)	Diamond Laboratory	NA
FITC anti-KLRG1	BioLegend	Cat # 138410
Alexa Fluor 700 anti-CD127	eBioSceince	Cat # 14-1278-82
Alexa Fluor 647 anti-IFNγ	BD BioScience	Cat # 557735
Anti-mouse CD16/32	eBioSceince	Cat # 14-0161-85
Fixable Viability Dye eFluor 506	Invitrogen	Cat # 65-0866-14
BUV395 anti-CD45	BD BioSciences	Cat # 564279
Pacific blue anti-CD62L	BioLegend	Cat # 104424
PE anti-CD44	BioLegend	Cat # 103024
PE/Cy7 anti-mouse anti-CD4	BioLegend	Cat # 100422
PerCP/Cy5.5 anti-CD8b	BioLegend	Cat # 126610
APC/Cy7 anti-CD19	BioLegend	Cat # 115530
Alexa Fluor 488 anti-CD3	BioLegend	Cat # 100210
Fixable Aqua dead cell stain	Invitrogen	Cat # L34965
BV 605 anti-TNFα	BioLegend	Cat # 506329
anti-CD8α	BioXcell	Cat # BE0117
Rat IgG2b isotype control	BioXcell	Cat # BE0090
HRP-conjugated goat anti-mouse IgG	Sigma Aldrich	Cat # A0168-1ML
Anti-Mouse IgG (γ-chain specific)−Biotin antibody	Sigma Alrich	Cat# B7022
PE anti-CD138	BD BioScience	Cat # 553714
Anti-PE microbeads	Miltenyi Biotec	Cat # 130-048-801
Bacterial and Virus Strains		
Zika virus Dakar clone 41525-mouse adapted	Diamond laboratory	Gorman et al., 2018
ZIKV H/PF/2013	X. de Lamballerie laboratory	Baronti et al., 2014
GAd-control (GC46Null)	Precigen	NA
Chemicals, Peptides, and Recombinant Proteins		
Recombinant ZIKV E protein	Meridian Life Science	Cat # R01635
ZIKV-derived, Db-restricted peptide E294-302	WU Center for Human Immunology	Elong Ngono et al., 2017
Recombinant ZIKV NS1 protein	Native Antigen	Cat # ZIKVSU-NS1
Critical Commercial Assays		
RNeasy mini kit	QIAGEN	74104
QIAamp viral RNA Mini kit	QIAGEN	52906
Taqman RNA-to-CT 1-step kit	Applied Biosystem	4392938
Fixation/Permeabilization solution kit	BD BioSciences	Cat # 554714
Mitomycin C from Streptomyces caespitosus	Sigma Aldrich	Cat # M4287
NP 40 Substitute	Sigma Aldrich	Cat # 74385
CD19 microbeads	Miltenyi Biotec	Cat # 130-052-201
1 step Fix/Lyse Solution	eBioSceince	Cat # 00-5333-54
Experimental Models: Cell Lines		
Vero	ATCC	CCL-81
A549	ATCC	CCL-185

(Continued on next page)

Continued

REAGENT or RESOURCE	SOURCE	IDENTIFIER
Experimental Models: Organisms/Strains		
C57BL/6J mice	Jackson Laboratory	000664
hSTAT2 KI mice	Diamond Laboratory	NA
C1q$^{-/-}$ mice	(Botto et al., 1998)	NA
Oligonucleotides		
ZIKV Dakar TaqMan primers	(Gorman et al., 2018)	NA
Recombinant DNA		
pACgc46E1(d2t.L)	Precigen	NA
pGC46CMVTetO.MCS.SV	Precigen	NA
ZIKV prM-E	Fremont Laboratory	GenBank Accession # KJ776791.2
Software and Algorithms		
Prism	Graphpad	Version 8.1.1
FlowJo	FlowJo, LLC	Version 10.0.7

LEAD CONTACT AND MATERIALS AVAILABILITY

Further information and requests for resources and reagents should be directed to and will be fulfilled by the Lead Contact author Michael S. Diamond (diamond@wusm.wustl.edu). All plasmids, antibodies, cells, viruses, and mouse lines developed for this study are available under Material Transfer Agreements from Washington University or Precigen.

EXPERIMENTAL MODEL AND SUBJECT DETAILS

Viruses and cells

ZIKV strain Dakar 41525 (Senegal, 1984, GenBank: KU955591) was provided by the World Reference center for Emerging Viruses and Arboviruses (R. Tesh and S. Weaver, University of Texas Medical Branch) and adapted by passage in *Rag1*$^{-/-}$ mice (Gorman et al., 2018). In some experiments, ZIKV strain H/PF/2013 (French Polynesia, 2013) was used (obtained from X. de Lamballerie, Aix Marseille Université). Virus stocks were propagated in Vero cells and titrated by focus-forming assay (FFA), as previously described (Lazear et al., 2016).

Mouse experiments

Animal studies were carried out in accordance with the recommendations in the Guide for the Care and Use of Laboratory Animals of the National Institutes of Health. The protocols were approved by the Institutional Animal Care and Use Committee at the Washington University School of Medicine (Assurance number A3381-01). Virus inoculations were performed under anesthesia that was induced and maintained with ketamine hydrochloride and xylazine, and all efforts were made to minimize animal suffering.

C57BL/6 mice were purchased from The Jackson Laboratory (catalog 000664), and congenic hSTAT2-KI (Gorman et al., 2018) and *C1q*$^{-/-}$ mice (Botto et al., 1998) were bred in pathogen-free animal facilities at Washington University School of Medicine. Immunizations were conducted by inoculating vaccines in 50 μl via intramuscular route. ZIKV challenges were performed by subcutaneous inoculation in the footpad with 3 × 10^5 FFU of mouse-adapted ZIKV Dakar 41525 in 30 μl of PBS. In some mice, ZIKV infections were preceded by administration of 2 mg of anti-Ifnar1 blocking antibody (MAR1-5A3, Leinco (I-1188)) via intraperitoneal injection. For pregnancy experiments, wild-type C57BL/6 or hSTAT2-KI female were mated with naive wild-type male mice or hSTAT2-KI males, respectively; at E5, pregnant dams (wild-type C57BL/6 mice only) were treated with a 2-mg injection of anti-Ifnar1 antibody. At E6, mice were inoculated with 10^5 FFU of mouse-adapted ZIKV Dakar 41525 by subcutaneous injection in the footpad. Animals were sacrificed at E13, and placentas, fetuses, and maternal tissues were harvested.

METHOD DETAILS

Construction and generation of GAd vectors

The genomes of GAd-Zvp and GAd-Eecto vectors were generated by homologous recombination using the plasmid pACgc46E1(d2t.L) containing the E1-deleted genome of GAd clone GC46 and the derivatives of shuttle plasmid pGC46CMVTetO.MCS.SV (plasmids provided by Precigen). Plasmids were transformed into *E. coli* strain BJ5183 as previously described (Duncan et al., 2013). The cDNA insert of GAd-Zvp was comprised of the IL-2 signal sequence, the coding region on

prM gene, the full-length E gene of ZIKV H/PF/2013 polyprotein (nucleotides 414-2429, Accession #; Baronti et al., 2014 KJ776791.2) and a stop codon (TGA); this construct was cloned into the shuttle plasmid pGC46CMVTetO.MCS.SV under transcriptional control of CMV promoter followed by an SV40 polyadenylation signal in place of E1 genes deleted in GAd genome. The cDNA insert of GAd-Eecto was comprised of the IL-2 signal sequence, the coding region on prM gene, the E gene lacking its transmembrane domain (nucleotides 414-2135 of ZIKV H/PF/2013) followed by a hexa-histidine tag and stop codon. The pGAd-Zvp and pGAd-Eecto plasmids were linearized with PmeI and transfected into M2A cells to rescue and upscale replication-incompetent GAd-Zvp or GAd-Eecto vectors (Gall et al., 2007). The E1-deleted vector GC46Null, which does not express any transgenes, was provided by Precigen and used as a negative control (GAd-control). Recombinant viruses were purified using cesium chloride density-gradient ultracentrifugation, and the number of virus particles (vp) was determined using optical density (260 nm) measurement as previously described (Mittereder et al., 1996). To confirm expression of the constructed ZIKV prM-Eecto and prM-E transgenes, A549 cells were mock-infected or infected with GAd-Zvp or GAd-Eecto vector at multiplicity of infection (MOI) of 1,000 virus particles/cell, and the presence of E protein in the supernatants of infected cells was examined 5 days post-infection by western blotting using an anti-ZIKV mAb (ZV-48; Zhao et al., 2016).

Negative staining and transmission electron microscopy

A549 cells were inoculated with GAd-Zvp or GAd-Eecto at a MOI of 1,000. The supernatants were harvested five days later, clarified by centrifugation at 4,000 rpm for 10 min at 4°C, loaded over a 20% w/v sucrose cushion in TNE buffer (10 mM Tris-HCl, pH 8.0, 120 mM NaCl and 1 mM EDTA), and pelleted by ultracentrifugation at 32,000 rpm at 4°C for 2 h. Purified VLPs were collected and imaged by electron microscopy. Samples were absorbed onto freshly glow discharged formvar/carbon-coated copper grids for 10 min. Grids were washed in dH$_2$O and stained with 1% aqueous uranyl acetate (Ted Pella Inc.) for 1 min. Excess liquid was wicked off gently, and grids were air-dried. Samples were viewed on a JEOL 1200EX transmission electron microscope (JEOL USA) equipped with an AMT 8 megapixel digital camera (Advanced Microscopy Techniques). The nominal magnifications used were 50,000, and 10,000. A ZIKV VLP preparation generated from 293T cells was used as a positive control.

ELISA

The ZIKV E-binding IgG responses were determined using an ELISA, as previously described (Zhao et al., 2016). Briefly, Maxisorp 96-well plates (Nunc) were coated with recombinant ZIKV E protein (Meridian Life Science Inc.) overnight at 4°C. On the next day, plates were washed extensively with PBS with 0.02% Tween 20 (PBS-T) and then blocked with 5% BSA in PBS-T for 1 h at 37°C. Serially diluted serum samples were added to the wells and incubated for 1 h at room temperature followed by washing and 1 h incubation with biotin-labeled goat anti-mouse IgG (Sigma) at room temperature. After additional washing, ZIKV E-binding IgG were detected using an HRP-conjugated streptavidin (1 h at room temperature) and tetramethylbenzidine substrate. The reaction was then stopped by addition of 1 N sulfuric acid and optical density (450 nm) measurements were determined using microplate reader (Bio-Rad). A similar ELISA was prepared with plates coated with recombinant ZIKV Eecto, DIII or DIII-LR mutant (A310E and T335K) (Zhao et al., 2016) to assess polyclonal antibody reactivity to the DIII-LR epitope. A simliar ELISA was conducted to determine serum anti-NS1 titers, with recombinant ZIKV NS1 (Native Antigen) used as the solid phase antigen.

Neutralization assay

A FRNT measured ZIKV neutralizing antibody, as previously described (Zhao et al., 2016). Briefly, heat-inactivated sera were serially diluted and incubated with 10^2 FFU of ZIKV (strain H/PF/2013) for 1 h at 37°C. The ZIKV-serum mixtures were added to Vero cell monolayers in 96-well plates and incubated for 1 h at 37°C followed by overlaying the cells with 1% (w/v) methylcellulose in MEM. Cells were incubated for 40 h and subsequently fixed using 1% PFA in PBS for 1 h at room temperature. ZIKV-infected cell foci were detected using anti-WNV E60 [(500 ng/ml), (Oliphant et al., 2006)] followed by horseradish-peroxidase-conjugated goat anti-mouse IgG (Sigma) in PBS supplemented with 0.1% (w/v) saponin (Sigma) and 0.1% BSA. TrueBlue peroxidase substrate (KPL) was used to develop the plates before counting the foci on a BioSpot analyzer (Cellular Technology Limited).

MBC limiting dilution assay

MBC responses were determined by measuring the levels of ZIKV E-specific IgG in the supernatants of CD19$^+$ B cells cocultured with NIH 3T3 feeder cells ectopically expressing CD40L, IL-21, and BAFF following protocols adapted from published papers (Amanna and Slifka, 2006). Single cell suspensions were prepared from spleens of immunized mice. Erythrocytes were lysed with ACK lysis buffer, and CD19$^+$ B cells were isolated by positive selection using magnetic beads (Miltenyi Biotec). Feeder cells were treated with 5 μg/mL of mitomycin (Sigma) to prevent proliferation, and CD19$^+$ B cells were cocultured in RPMI supplemented with 10% FBS, penicillin and streptomycin, 10 mM HEPES pH 7.3, 50 μM β-mercaptoethanol, and 10 mM nonessential amino acids, in a twofold serial dilution starting at 10^6 cells/well in a 96-well plate. Plates were incubated at 37°C in a CO$_2$ incubator for 6 days. The frequencies of ZIKV E-specific MBC were determined using an ELISA for ZIKV E-specific IgG as described above and Poisson distribution analysis. Positive wells were defined as wells that scored twofold over the mean optical density of negative control wells (wells containing irradiated splenocytes and supplements alone). Supernatant from cultured naive splenocytes did not score positive, and only limiting dilution assays that contained at least two positive wells at the highest dilution were analyzed.

ELISPOT assay

An ELISPOT assay quantitated the number of ZIKV E-specific LLPCs in the bone marrow, as previously described (Purtha et al., 2011). ELISPOT plates (Millipore) were coated with ZIKV E protein overnight at 4°C. Subsequently, plates were washed twice with PBS-T, then twice with PBS and then blocked for 1-3 h with RPMI supplemented with 10% FBS, penicillin and streptomycin, 10 mM HEPES pH 7.3, 50 μM β-mercaptoethanol, and 10 mM nonessential amino acids (RPMI-Complete). Bone marrow cells were harvested from the femurs of immunized mice, and erythrocytes were lysed by ACK lysis buffer. Subsequently, CD138$^+$ plasma cells were enriched by positive selection using magnetic beads (Miltenyi Biotec), resuspended in RPMI-Complete at 10^7 cells/ml, serially diluted in the coated ELISPOT plates, and incubated overnight at 37°C in a CO$_2$ incubator. Plates then were washed five times with PBS, incubated with 1% NP40 in PBS for 20 min at room temperature, and washed three times with PBS-T. Plates were incubated with biotinylated anti-mouse IgG (Sigma) in PBS-T with 1% FBS for 1 h at room temperature. Following washing with PBS-T, plates were incubated with HRP-conjugated streptavidin (1 h at room temperature). Spots were developed with trueBlue peroxidase substrate (KPL) before the reaction was quenched with water and counted with a BioSpot analyzer (Cellular Technology Limited).

Measurement of viral burden

ZIKV-infected mice were euthanized using a ketamine/xylazine cocktail on the indicated days post-infection, and blood and organs were collected. Serum was separated from coagulated blood, and tissues were weighed and homogenized with beads using a MAgNA Lyser (Roche). RNA was extracted using RNeasy Mini Kit or RNeasy 96 kit (QIAGEN). Viral RNA levels were measured using TaqMan one-step quantitative reverse transcriptase PCR (RT-qPCR) on an ABI 7500, after comparison with a standard curve generated using 10-fold serial dilution of viral RNA from known infectious virus quantities. Viral burdens were expressed as viral RNA equivalents per gram or milliliter on a log$_{10}$ scale. For RT-qPCR, published ZIKV primers and probe set were used (Richner et al., 2017a): Forward 5'-CCACCAATGTTCTCTTGCAGACATATTG-3'; Reverse 5'- TTCGGACAGCCGTTGTCCAACACAAG-3'; Probe 5'-/56 FAM/ AGCCTACCT/ZEN/TGACAAGCAGTC/3IABkFQ/-3' (Integrated DNA Technologies).

Intracellular Cytokine Staining

Freshly-isolated mouse splenocytes were stimulated with an H-2D^b-restricted immunodominant ZIKV peptide (amino acids 294-302), with rat anti-mouse CD3 used as a positive control and medium as negative control, for 12 h at 37°C before brefeldin A (BioLegend, 420601) was added for an additional 4 h. Subsequently, single-cell suspensions were blocked for FcγR binding (BioLegend; clone 93) and stained with the following antibodies: CD45 BUV395 (BD BioSciences clone30-F11), CD62L Pacific Blue, KLRG1 FITC, CD44 PE, CD4 PE-Cy7, CD8b PreCP-Cy5.5, CD19 APC-Cy7 (BioLegend clones MEL-14, 2F1/KLRG1, IM7, GK1.5, YTS156.7.7, 6D5, respectively), CD127 Alexa700 (eBioScience clone A7R34), and fixable viability dye (eFluor 506, eBioscience). Subsequently, cells were fixed and permeabilized with Foxp3/Transcription Factor Staining Buffer Set (eBiosciences, 00-5523-00) followed by intracellular staining with anti-TNF-α BV605 and anti-IFN-γ Alexa 647 (BD Biosceinces clones MP6-XT22 and XMG1.2, respectively). Datasets were acquired on a LSRII flow cytometer and analyzed using FlowJo software X 10.0.7.

CD8$^+$ T cell depletion

To deplete CD8$^+$ T cells, anti-CD8α (BioXCell; clone YTS169.4; 500 μg) or an isotype control (BioXCell; clone LTF-2; 500 μg) was administered to immunized mice by intraperitoneal injection at days −7, −3, +1, +5 and +12. Mice then were challenged with 3 × 10^5 FFU of mouse-adapted ZIKV Dakar (41525) at day 0 that was preceded by intraperitoneal inoculation of anti-ifnar1 blocking mAb. To confirm immune cell depletion, peripheral blood was collected at 7 dpi followed by erythrocyte lysis with ACK lysis buffer (GIBCO) and resuspension in RPMI supplemented with 10% heat-inactivated FBS. Cells were blocked for FcγR binding and stained with CD45 BUV395 (BD BioSciences clone30-F11), CD3 Alexa488 (BioLegend clone1452C11), CD4 PE-Cy7 (BioLegend clone GK1.5), CD8b PreCP-Cy5.5 (BioLegend clone YTS156.7.7), and Fixable Aqua Dead Cell Stain (Invitrogen, L34966). Subsequently, cells were fixed by Fix/Lyse solution (eBioSciences 00-5333). Datasets were acquired on a LSRII flow cytometer and analyzed using FlowJo software X 10.0.7.

QUANTIFICATION AND STATISTICAL ANALYSIS

Specific statistical tests used to analyze experimental datasets are described in the respective Figure Legends. For antibody responses and immune cell analyses, one-way ANOVA with Dunn's or Dunnett's post-test was used. For viral titer data analysis, a Mann–Whitney test or a Kruskal–Wallis ANOVA with Dunn's post-test correction was used. Survival curves were analyzed using the log rank test with a Bonferroni correction, and weight change was evaluated with a two-way ANOVA with a Dunnett's post-test or with two-way ANOVA with Sidak's post-test correction. A P value of < 0.05 was assigned to establish statistical significance using GraphPad Prism version 7.0.

DATA AND CODE AVAILABILITY

The published article includes all data generated or analyzed during this study. Original source data for Figures in the paper are available upon request to the Lead Contact author. No proprietary software was used in the data analysis.

Supplemental Information

A Gorilla Adenovirus-Based Vaccine

against Zika Virus Induces Durable Immunity

and Confers Protection in Pregnancy

Ahmed O. Hassan, Igor P. Dmitriev, Elena A. Kashentseva, Haiyan Zhao, Douglas E. Brough, Daved H. Fremont, David T. Curiel, and Michael S. Diamond

Table S1. Evaluation of ZIKV vaccine platforms in mice, Related to all Figures

Vaccine platform	Vaccine Efficacy in mice				Reference
	# Doses	Neutralization titer	Protection against ZIKV challenge	Protection against *in utero* transmission	
Gorilla adenovirus encoding prM-E (GAd-Zvp)	1 or 2	FRNT EC_{50} $1,796 \pm 919$	Yes (No viremia or lethality)	Yes	This study
Ad26.ZIKV.M-Env	1	FRNT EC_{50} ~ 1,000	Yes (No viremia)	N.D.*	(Cox et al., 2018)
Chimpanzee adenovirus type 7 (AdC7-M/E)	1	MN_{50} ~1,000	Yes (No viremia or lethality)	N.D.	(Xu et al., 2018)
mRNA encoding prM-E	2	FRNT EC_{50} 10,000	Yes (No lethality)	Yes	(Richner et al., 2017a, 2017b)
DNA encoding prM-E	1	MN_{50} 22	Yes (No viremia)	N.D.	(Larocca et al., 2016)
DNA encoding E	1	NN_{50} <10	No (viremia detected)	N.D.	(Larocca et al., 2016)
Measles-vectored prM-Zika-sE	2	$PRNT_{50}$ 40 - 1,280	Yes (Viremia and organ viral loads reduced)	Yes **	(Nürnberger et al., 2018)
ZIKV-3′UTR-Δ10-LAV (live attenuated)	1	FRNT EC_{50} $18,900 \pm 5,900$	Yes (No lethality)	Yes	(Shan et al., 2017a, 2017b)
DNA encoding prM-E	1	$PRNT_{50}$ 456 ± 5	Yes (No lethality)	N.D.	(Muthumani et al., 2016)

DNA encoding prM-E	1	RVP ~1000-100000	ND	N.D.	(Dowd et al., 2016)
Purified inactivated virus	1	MN$_{50}$ 15	Yes (No viremia)	N.D.	(Larocca et al., 2016)
hAd2-vecored prM-E, prM-E-NS1	2	MN$_{50}$ ~1,000	Yes***	N.D.	(Liu et al., 2018)

*N.D. = not determined; FRNT, focus reduction neutralization test; PRNT, plaque reduction neutralization test; MN, microneutralization test; RVP, reporter virus particles.

** Reduced viremia and viral loads in fetuses and maternal tissues

*** Challenge in pups born to immunized dams showed reduced viral loads in brain and testis